New Experimental Data and Reference Models for the Viscosity and Density of Squalane

Kurt A. G. Schmidt[*1], Doug Pagnutti[2], Meghan D. Curran[3], Anil Singh[4], J. P. Martin Trusler[5], Geoffrey C. Maitland[5], Mark McBride-Wright[5]

Affiliation:

[1]Schlumberger, Abingdon Technology Center, Lambourn Court, Wyndyke Furlong, Abingdon, United Kingdom, OX14 1UJ

[2] Schlumberger, DBR Technology Center, 9450-17 Ave, Edmonton, AB, Canada, T6N 1M9

[3]Department of Chemical and Materials Engineering, University of Alberta, 9107 - 116 Street, Edmonton, AB, Canada, T6G 2V4

[4]Schlumberger, Schlumberger Rosharon Campus, 14910 Airline Road, Rosharon, TX, USA, 77583

[5]Department of Chemical Engineering, Imperial College London, South Kensington Campus, London, United Kingdom, SW7 2AZ

*Corresponding Author E-mail: kschmidt@slb.com

ABSTRACT

Empirical models for the density and the viscosity of squalane ($C_{30}H_{62}$; 2,6,10,15,19,23-hexamethyltetracosane) have been developed based on an exhaustive review of the data available in the literature and new experimental density and viscosity measurements carried out as a part of this work. The literature review showed there was a substantial lack of density and viscosity data at high temperature (373 to 473) K and high pressure conditions (pressures up to 200 MPa). These gaps were addressed with new experimental measurements carried out at temperatures of (338 to 473) K and at pressures of (1 to 202.1) MPa. The new data were utilized in the model development to improve the density and viscosity calculation of squalane at all conditions including high temperatures and high pressures.

The model presented in this work reproduces the best squalane density and viscosity data available based on a new combined outlier and regression algorithm. The combination of the empirical models and the regression approach resulted in models which could reproduce the experimental density data with average absolute percent deviation of 0.04%, bias of 0.000%, standard deviation of 0.05%, and maximum absolute percent deviation of 0.14% and reproduce the experimental viscosity data with average absolute percent deviation of 1.4%, bias of 0.02%, standard deviation of 1.8% and maximum absolute percent deviation of 4.9% over a wide range of temperatures and pressures. Based on the data set used in the model regression (without outliers), the density model is limited to the pressure and temperature ranges of (0.1 to 202.1) MPa and (273 to 525) K, while the viscosity model is limited to the pressure and temperature ranges of (0.1 to 467.0) MPa and (273 to 473) K. These models can be used to calibrate laboratory densitometers and viscometers at relevant high-temperature, high-pressure conditions.

Keywords: Squalane, Viscosity, Density, Correlation, HTHP conditions

1. INTRODUCTION

The viscosity of reservoir fluids is an important property in all aspects of reservoir production and it, along with its associated uncertainty, affects engineering design decisions. Reservoirs are currently being developed with increasingly elevated temperatures and pressures and with highly viscous fluids. Ultra-deep Gulf of Mexico offshore prospects and bitumen reserve extraction from oil sands are examples of areas where High Pressure (HP) and/or High Temperatures (HT) conditions and viscous fluids exist.

The viscosity of reservoir fluids is routinely measured in commercial laboratories with capillary and falling body viscometers. These viscometers are typically calibrated at atmospheric conditions and specific temperatures with standard calibration fluids. Calibrations are then extended to elevated pressure and temperature conditions with empirical correlations or the viscometer is calibrated at limited temperature and pressure conditions with available HTHP reference fluids. To lower the uncertainty of routine viscosity measurements, viscometers require accurate calibrations and/or reference fluids to verify equipment calibrations. The measurement of viscosity also requires accurate densities at the same conditions.

Unfortunately, most current viscosity standards are inadequate for supporting improved experimental accuracies in HTHP and high viscosity fluid environments. Squalane ($C_{30}H_{62}$; 2,6,10,15,19,23-hexamethyltetracosane), a pure fluid of moderate viscosity, has been identified to fill the gap between existing reference fluids and potential HTHP and high viscosity standards. During the fluid selection process, a critical analysis of existing squalane literature identified voids and discrepancies in the existing data sets. New experimental measurements were performed to fill these voids and these new data were combined with existing literature data to determine new reference equations for the viscosity and density of pure squalane.

The parameters in the developed models for viscosity and density were determined with a novel approach for robust regression which combined global optimization and outlier detection algorithms. The overall algorithm, combined with the critical literature review, provided a recommended data set, a reliable set of parameters, and a range of validity for the models.

2. LITERATURE REVIEW

Development of accurate viscosity and density models requires a thorough knowledge of existing literature data and the acquisition of new experimental measurements to fill the void in the existing data sets. There are numerous data sets for the density and viscosity of squalane and they have been reviewed and an analysis of the published results has been performed. A complete list of the literature data sets used in this investigation is presented in Tables 1 and 2. This compilation of data indicated that additional measurements at high temperature and high pressure conditions were needed to fill voids in the available literature. Accordingly, new measurements were performed at temperatures in the range of (338 to 473) K and at pressures between (0.2 and 202.1) MPa; the results are presented in this paper. These new data and the derived models helped to resolve discrepancies between existing data sets and to extend regions where the physical properties were insufficiently modelled with the correlations presented in the literature to this date.

References with tabulated data were considered and those which presented data in only Figures were excluded.[43-52] In cases where an existing experimental data set was repeated (or it appeared that the same point was not re-measured) in subsequent articles, only the original data set was included in the regression data set: Lal et al. (2000)[18,21,53-54], Dubey and Sharma (2008)[24,55-59], Bair (2002)[36-37], Whitmore et al. (1966)[8,60], Cadogan and Purnell (1969)[9-10,61], Kumagai et al. (2006)[22,62].

Unlike the works by Schmidt et al. (2008)[63] and Quiñones-Cisneros et al. (2012)[64], where there was a very limited data set available for the development of a reference model, the abundance of experimental data for squalane made it unnecessary to include molecular simulations in this work.[37,65-73] Two points from Whitmore et al. (1966)[8] were not included due to the inability of converting kinematic viscosities of sub-cooled squalane (219 and 233) K.

The data sets presented in Tables 1 and 2, which include the new measurements described in the following section, span large temperature and pressure ranges and provided sufficient information to develop a versatile model which can be used in most laboratory settings as a calibration tool. Plots showing the range of the available density and viscosity data, as a function of pressure and temperature, are presented in Figures 1 and 2. As can be seen in both figures, the new data significantly extends the range of data available for model development.

3. EXPERIMENTAL METHOD FOR DENSITY AND VISCOSITY MEASUREMENTS

The measurements were made using a vibrating-wire apparatus that provides simultaneous measurements of viscosity and density.[74-76] As illustrated in Figure 3, the vibrating wire is suspended vertically in the fluid, between the poles of a permanent magnet, and is tensioned by an aluminium weight. An alternating current is passed through the wire, thereby setting it into transverse oscillation, and the electromotive force (emf) developed across the wire is measured by means of a lock-in amplifier. This emf generally comprises two components: the first is simply the voltage developed across the electrical impedance presented by the stationary wire; while the second is the induced voltage arising from the motion of the wire through the fluid in the presence of the magnetic field. The frequency response of the oscillating wire is measured in the vicinity of the fundamental transverse resonance mode. The resonance frequency of this mode is sensitive to the density of the surrounding fluid, largely as a consequence of the buoyancy effect exerted on the weight and the resulting changes in the tension of the wire. The width of the resonance curve is sensitive to the viscosity of the fluid. Both effects are described accurately by a full-developed working equation for the instrument.[74,77-80] The practical apparatus and standard operating procedures are described in detail by Ciotta (2010).[76]

With a tungsten wire of 0.15 mm diameter fitted for this project, the instrument had a nominal working range for viscosity of approximately (0.5 to 100) mPa·s.

4. CALIBRATION

In the present work, viscosity measurements were made in an absolute way without the need to calibrate the instrument in a fluid of known viscosity. This was achieved by measuring the diameter of the wire with a laser micrometer. The wire used was centreless-ground tungsten (Metal Cutting Corp., New Jersey, USA) with a nominal diameter of 0.15 mm. The diameter of the actual piece used was measured by means of the laser micrometer (Aeroel SRL, Pradamano, Italy) with 0.01 µm

resolution. Measurements were made at three different axial positions and at five different angles and the results are given in Table 3. The mean diameter obtained was 0.15112 mm, with a standard deviation of 0.00009 mm and min/max deviations of -0.00015 mm and 0.00012 mm. This result is in essentially exact agreement with the value of 0.1511 mm stated by the supplier.

The remaining parameters in the working equation pertain to the resonance frequency of the wire and these were determined, as described recently,[80] from calibration measurements in air at ambient pressure.

The temperature of the vibrating-wire cell was measured with a platinum resistance thermometer (PRT) probe having a nominal resistance of 100 Ω at T = 273.15 K. The resistance of the thermometer was measured in a four-wire circuit using a digital multimeter (Agilent, model 34401A). The thermometer was previously calibrated both in a water triple-point cell and by comparison with a standard PRT in an oil bath at temperatures between 323 K and 473 K.[76] The standard PRT used for this purpose (Tinsley, model B249) had itself been calibrated on ITS-90 by the UK National Physical Laboratory. At the conclusion of the present study the PRT was checked again in a triple point of water cell and its resistance was found to be unchanged. The estimated standard uncertainty of the temperature was ±0.02 K.

The pressure was measured by means of a Paroscientific Digiquartz transducer (model number 430K-110) with a range of (0 to 207) MPa calibrated by the supplier against a certified pressure balance. After allowing for the offset observed under vacuum, the estimated standard uncertainty of the pressure measurements was ±0.02 MPa.

5. MEASUREMENT PROGRAMME

The provenance and purity of the squalane sample (CAS 111-01-3) is provided in Table 4 and no further purification of the sample was attempted. The entire apparatus was evacuated before introducing the sample. About 200 ml of sample was transferred to a glass reservoir fitted with a close-fitting screw cap and a dip tube through which sample could be withdrawn. The dip tube was connected to the inlet of the high-pressure fluid handling system and the fluid was drawn into the evacuated system. The fluid handling system was then used to pass approximately 50 ml of sample through the apparatus for flushing purposes. Pressure was raised by means of a screw injector in the fluid handling system.

The measurements were made along isotherms with actual temperatures within 0.2 K of the desired nominal values. In order to characterise the isotherms well, an initial point close to 1 MPa was measured, followed by 20 MPa and then increments of 20 MPa until the pressure reached approximately 200 MPa; the pressure was then reduced to a value close to 1 MPa for a check measurement. The actual temperatures and pressures were measured as detailed in section 4 above. At each state point, at least two measurements were made and the resulting values averaged. Normally, the repeatability at a constant temperature and pressure was within 0.5 % in viscosity and 0.05 % in density. There was increased scatter at viscosities above about 30 mPa·s increasing to about ± 1 % in viscosity and ± 0.5 % in density at η = 100 mPa·s. In these cases, the number of repeated measurements was increased to 5 leading to a standard error of the mean of about 0.5 % in viscosity and 0.25 % in density. The estimated overall expanded uncertainties, taking

account of all sources of uncertainty other than sample degradation, were 2 % for viscosity and 0.2 % for density, with a coverage factor of 2.

One problem that arose was premature failure of the rupture-disc safety device after the measurement at 453 K and 180 MPa. The rapid decompression of the system that occurred when the disc ruptured caused damage to the sensor lead wires and also caused the sinker to slip on the lower end of the vibrating wire. The system was repaired and the sinker replaced. Check measurements overlapping the previous data were made after this repair and before continuing; the check results showed good agreement.

6. VERIFICATION TESTS

In order to test the measurement system, measurements were made on the viscosity standard liquid S20 (Cannon Instrument Co.) at temperatures of (298.15, 323.15 and 353.15) K and at ambient pressure. The results were compared with the values certified by the supplier and the results are given in Table 5; small corrections were applied to account for deviations (< 0.2 K) from the nominal temperatures. The measured viscosity agrees with the certified values of the viscosity standard liquid to well within the overall experimental uncertainty. The measured densities are approximately 0.3 % lower than the certified values and these differences fall slightly outside the 95 % confidence interval of ±0.2 %. There is no explanation for this discrepancy.

In further tests, a u-tube capillary viscometer (PSL BS/U D serial number 55281) was used to measure the kinematic viscosity μ of both fresh squalane and used squalane drained from the vibrating-wire instrument after the final measurements at T = 473.15 K. The u-tube viscometer was operated at ambient pressure and was immersed in a temperature-controlled water bath. The overall standard relative uncertainty of these measurements was ±0.2 %. The densities of the same samples were measured in an Anton Paar DMA 5000 vibrating-tube densimeter with automatic viscosity correction and an overall standard relative uncertainty of 0.01 %. The DMA 5000 was calibrated in ambient air and ultrapure water at the operating temperature. In order to facilitate comparison with the vibrating-wire results, the density and the logarithm of the viscosity measured along the isotherm at T = 338 K and $P \leq 101$ MPa were each extrapolated to $P = P_0$, where P_0 = 0.1 MPa, by means of linear regression with a quadratic polynomial in $(P - P_0)$. These quadratic polynomials provided excellent fits and led to η = (6.706 ± 0.003) mPa·s and ρ = (778.5 ± 0.3) kg·m^{-3} at P = 0.1 MPa and T = 338 K, where the quoted uncertainties are one standard deviation. A preliminary surface fit that $(\partial \ln\eta/\partial T)_P$ = -0.026 K^{-1} and $(\partial \ln\rho/\partial T)_P$ = -0.00084 K^{-1} at the same pressure and temperature was also estimated. These derivatives were used to correct the values of η and ρ extrapolated from the vibrating-wire measurements to the slightly different temperatures at which the ambient-pressure measurements were made. In Table 6, the results of the ambient-pressure measurements and the differences $\Delta\eta$ and $\Delta\rho$ from the values deduced from the vibrating-wire data are presented. Both the capillary viscosity measurements agree well with the vibrating-wire results but there is a small difference between them that suggest some degradation of the sample after exposure to the highest experimental temperature. This correlates with a slight discolouration of the used fluid noted after the final isotherm. In this case, the densities are found to agree to well within the 95 % confidence interval.

7. EXPERIMENTAL RESULTS

The measured viscosity and density of squalane are given in Table 7 in the original order of the measurements. The results are plotted in Figures 4 and 5.

8. DENSITY AND VISCOSITY MODEL

The modified Tait Equation,[81] has been widely used to correlate the (*P*,*ρ*,*T*) surface of numerous pure fluids and mixtures including squalane.[26]

$$\rho / (\mathrm{kg \cdot m^{-3}}) = \rho_0 \left[1 - C \log_{10} \left(\frac{P + B}{P_0 + B} \right) \right]^{-1} \quad (0)$$

where the reference density, ρ_0, is the density of squalane at P_0 = 0.1 MPa. The parameter *C* is a constant and *B* is a parameter with temperature dependency described in Equation (2):

$$B / \mathrm{MPa} = \sum_{i=0}^{2} b_i (T / \mathrm{K})^i \quad (0)$$

The reference density, ρ_0, was correlated as a function of temperature with Equation (3):

$$\rho_0 / (\mathrm{kg \cdot m^{-3}}) = \sum_{i=0}^{2} a_i (T / \mathrm{K})^i \quad (0)$$

A modified Tait-like viscosity equation (Comuñas, 2001)[82] was used to correlate the viscosity data

$$\eta = \eta_0 \left(\frac{P + E_\eta}{P_0 + E_\eta} \right)^{D_\eta} \quad (0)$$

where the reference viscosity, η_0, was described with a modified Andrade equation[82]:

$$\eta_0 = A_\eta \exp\left(\frac{B_\eta}{T + C_\eta} \right) \quad (0)$$

The reference pressure, P_0, in Equation(4) are the same as in Equation (1). Parameters, D_η, and E_η, were considered functions of temperature:

$$D_\eta = \sum_{i=0}^{2} d_i (\mathrm{K} / T)^i \quad (0)$$

$$E_\eta / \mathrm{MPa} = \sum_{i=0}^{2} e_i (T / \mathrm{K})^i \quad (0)$$

The density parameters to be regressed are therefore $\{a_0, a_1, a_2, b_0, b_1, b_2, C\}$ and the viscosity parameters are $\{A_\eta, B_\eta, C_\eta, d_0, d_1, d_2, e_0, e_1, e_2\}$.

9. PARAMETER DETERMINATION

The standard approach for determining equation parameters is to minimize the sum of squares of the residuals as described by Equation (8), known as the least-squares approach to regression.

$$\boldsymbol{c}_{\text{Least-Squares}} = \arg\min_{\boldsymbol{c}} \sum_i \left(y_i - f(x_i, \boldsymbol{c}) \right)^2 \tag{0}$$

Where $\mathbf{c}$ is the parameter vector, f is the model function and (x_i, y_i) are the experimental data.

Using this approach on the squalane data set leads to erroneous values due to the failure of two key assumptions made in the method's derivation[83]: 1) that the difference between the measured values and the actual values are all normally distributed, and 2) that all the data are valid for the chosen model (i.e. no outliers). The first assumption fails because the viscosity data spans several orders of magnitude and it is unreasonable to assume that the experimental uncertainty remains constant in absolute terms. Such an assumption would lead to a surface that fits the higher magnitude data at the expense of all the other values. The second assumption fails primarily because the model Equations (1) and (4) are empirically based and have a limited range of applicability but also because the different measurement techniques can lead to some points having significantly higher variance than others.

Instead, the least squares approach was changed so that: 1) the relative differences between the measured values and the model values are normally distributed and 2) there are a specific number of data points that should not be considered when determining the parameters and those points can be identified by the Benjamini-Hochberg test for significance.[84] This method of outlier detection was selected because it is based on the same *a priori* assumption of normally distributed data as the regression technique and there are enough data points that a more conservative method is not required.

The relative difference r_i between the measured value and the model function is given by Equation (9):

$$r_i = \frac{y_i - f(x_i, \boldsymbol{c})}{\sqrt{\left| \left(y_i \right) f(x_i, \boldsymbol{c}) \right|}} \tag{0}$$

This leads to the regression Equation (10) which is used by Weiland et al. (1993)[85]:

$$\boldsymbol{c}_{\text{Relative Difference Regression}} = \arg\min_{\boldsymbol{c}} \sum_i \frac{\left(y_i - f(x_i, \boldsymbol{c}) \right)^2}{\left| \left(y_i \right) f(x_i, \boldsymbol{c}) \right|} \tag{0}$$

This formulation, Equation (10), of the relative difference is preferable to the standard definition, given by Equation (11), as it has no bias:

$$r_i = \frac{y_i - f(x_i, \boldsymbol{c})}{y_i} \tag{0}$$

and it is a function which weights all of the data equally irrespective of the magnitude of the data (which in this case span several orders of magnitude). If *M* experimental measurements out of *N* total measurements are excluded, then the final regression equation is given by:

$$\boldsymbol{c}_{\text{Robust Regression}} = \arg\min_{\boldsymbol{c}} \sum_{i=1}^{N-M} \frac{\left(\tilde{y}_i - f(\tilde{x}_i, \boldsymbol{c})\right)^2}{\left|\left(\tilde{y}_i\right) f(\tilde{x}_i, \boldsymbol{c})\right|} \tag{0}$$

where $\tilde{}$ denotes that the measurement values have been sorted by increasing statistical significance.

10. REGRESSION IMPLEMENTATION

Evaluating Equation (12) is not trivial since the parameter vector $\mathbf{c}$ is highly dependent on the value *M* and the sorting of the values $\left(\tilde{x}_i, \tilde{y}_i\right)$ which in turn can only be determined once $\mathbf{c}$ is known. The solution procedure developed is an iterative process of choosing *M*, finding the parameters that minimize Equation (12), then using that equation to get a new estimate for *M* and repeating until *M* converges. Even with *M* known, Equation (12) is still difficult to solve as there can be many local minima that differ greatly from the global minimum. A further complication of the regression is the residuals used in each calculation can change (due to a change in order) and the parameter surface to be minimized can be highly discontinuous. The global minimization strategy, differential evolution[82], is able to reliably solve this problem as it can search over a large parameter space and does not require a continuous surface. The entire implementation is illustrated in Figure 6.

To perform the Benjamini-Hochberg significance test, the residuals are assumed to be normally distributed around zero with variance determined by the median absolute deviation, which is a robust variance estimator. The p-values P_i are then computed for each residual and the largest p-value that satisfies the significance test in Equation (13) is considered an outlier as well as all residuals with lower p-values.

$$P_i \leq \frac{i}{N+1-i}\alpha \tag{0}$$

The variable α is the false discovery rate, which is set at 5% by convention[84].

11. RESULTS AND DISCUSSION

To illustrate the improved parameter choice calculated using this novel approach to regression, the parameters of Equation (4) were computed using least squares regression, Equation (8), the modified objective function, Equation (10), and finally the full robust regression, Equation (12). The intersection of the resulting surfaces with the atmospheric pressure plane and the experimental viscosity data at atmospheric pressure are shown in Figure 7. It is noted that only the atmospheric pressure data is shown in Figure 7 even though the experimental data at atmospheric and elevated pressures were used in the regressions.

As can be seen in Figure 7, the least squares regression technique provides a poor fit of the atmospheric pressure data. The viscosity data at these conditions are being neglected in order to satisfy the objective function which favours the large viscosities at elevated pressures. This deficiency is clearly addressed by using the relative objective function. At atmospheric pressure, the regressed equation's performance is indistinguishable from that obtained with the robust regression. The histograms in Figures 8 and 9 show the distribution of the Absolute Percentage Deviation (APD, denoted Δ_i) of all the data points,

$$\Delta_i = 100\left|\frac{y_i - f(x_i, \boldsymbol{c})}{y_i}\right| \tag{0}$$

between the models and the density and viscosity data (all data - atmospheric and elevated pressures). An examination of the results show that the relative objective function does not result in a half-normal distribution of the errors as expected. A large number of points with deviations significantly greater than the majority of the differences between the model and the data set indicate that the presence of these outliers could skew the results. Use of the robust regression technique improves the parameterization of the model because the data points with significant deviations are excluded from the regression. As shown in Figures 8 and 9, the resulting deviation distribution for the robust regression and the identified outliers show that the deviations of the points used in the regression are significantly reduced; and now resemble more of a half-normal distribution when compared to the conventional regression technique (both with the relative difference objective function).

The optimal parameters and a summary of the regression's statistics for the viscosity and density can be found in Table 8. Out of a total of 853 viscosity points available in the literature, 97 (11 %) were considered outliers which is lower, on a percentage basis, than the number of density point outliers, 64 out of 407, or 16 %.

Overall, the average absolute percentage deviation (AAPD, denoted Δ),

$$\Delta = \frac{100}{N}\sum_{i=1}^{N}\left|\frac{y_i - f(x_i, \boldsymbol{c})}{y_i}\right| \tag{0}$$

between the optimal model and that of the data used in the parameterization (i.e. data points not rejected) is 0.04 % for the density and 1.4 % for the viscosity. The bias of the density fit is 0.000 % and the standard deviation is 0.05 %. The bias of the viscosity fit is 0.02 % and the standard deviation is 1.8 %. The bias and the standard deviation of the models are artificially reduced due to the rejection of the extreme 5% of valid points (set by the false discovery rate). With this considered, the maximum absolute percent deviation of these models is a good indicator of the goodness of fit of these models. The maximum APD of the density and viscosity points used in the regression was 0.14 % and 4.9 %. Based on the rejected data in the model regression, the density model is limited to the pressure and temperature ranges of (0.1 to 202.1) MPa and (273 to 525) K, respectively. As shown in Table 8, the lowest temperature in the accepted viscosity data set was 242.7 K. A review of this data set revelled that the majority of the accepted experimental measurements were made at temperatures of 273 K or greater. Based on this, the viscosity model is limited to the pressure and temperature ranges of (0.1 to 467.0) MPa and (273 to 473) K, respectively. The model is still useable

at temperatures between 243 and 273 K, but it has only been validated by significant quantities of experimental data down to 273 K. As with most empirical models, extrapolation of the models beyond the ranges described above is not recommended. Further details of the number of points used from each literature source and the AAPDs between the optimal models are presented in Tables 9 and 10. Most of the rejected viscosity data are at pressures greater than 500 MPa.

Tables 9 and 10 show the individual data sets used in the regression of the parameters for the recommended model. As can be seen in Table 9, most of the density data before 1957 was classified as outliers. This is consistent with the review of the data sets which indicated that these literature data sets do not report the experimental method or uncertainty of the measurements. More recent data sets[15,23,26] had a majority of points deemed as outliers. These outlier points appear to be inconsistent with the remaining literature data (including the new data). Tables 9 and 10 show that the AAPD of the rejected points were significantly larger than the points which appear to be consistent with the other data sets based on the model and the regressed parameters. The majority of the density data can be fit very well by the model (75% of points with error less than 0.1%), and therefore the tolerance for being considered a valid point is very tight and hence why some of the data may appear to be inconsistent with the model and other data sets.

Compared to the density data, the viscosity of squalane has been measured at significantly higher pressures (up to 1.298 GPa). Most of the data deemed outliers were at pressures greater than 400 MPa (and essentially all the data above 500 MPa). The data at pressures greater than 500 MPa came from Bair (2002)[36] and Bair (2006)[39]. Table 10 shows that the regression algorithm considered 50 out of the 78 points from these papers as outliers. Whether these points are experimentally consistent with the other data sets is difficult to ascertain from the results presented in this investigation. Based on the regression algorithm, the other experimental data sets, and the Tait-like viscosity model (9 parameters), the data appear to be inconsistent with those reported in the literature. Either the model is insufficient at these conditions or the data are inconsistent with the other data sets and the model. Further exploration into the consistency of these measurements, which are at extreme pressure conditions, was not performed. These extreme pressures are far from those which are measured in commercial laboratories (and most academic laboratories) and were considered outside scope of this work.

The compilation of data presented in this work could be used to further the development of a new squalane viscosity model which covers these extreme pressures. However, new data at these conditions should be measured at these conditions to verify the existing data before any modelling effort is undertaken. Although the data at these elevated conditions were not of practical interest for the model development in this work, they were still used in the determination of the model parameters. The success of this algorithm is proven by the development of a consistent model which was not biased by the data at these conditions. At pressures below 500 MPa, most of the data set from Krahn and Luft (1994)[35] appear to be inconsistent with those from the other investigators. In this case most of the data at elevated temperatures (greater than 293.15 K) were considered outliers.

Figure 10 shows the relative deviation of the measured density at atmospheric pressure from the correlating equations with the parameters given in Table 8. Figure 11 shows the relative deviation of the measured density as a function of pressure for all temperatures. The majority of the deviations

are within 0.1 % of the correlation for density. Figure 12 shows the relative deviation of the measured viscosity at atmospheric pressure and a majority of deviations are noted to be within 3 %. Figure 13 shows the relative deviation of the measured viscosity as a function of pressure for all temperatures. The majority of the deviations are within 5 % of the correlation for viscosity. Only data that were used in the parameterization have been included in these figures.

Very recently, Mylona et al.[28] have published correlations of the density and viscosity of squalane based on their analysis of the available experimental data, including the new data presented in this paper. In their work, the density was correlated using the same model as in the present analysis; however, they set $a_2 = 0$ and constrained C to the value 0.2. The region in which both density correlations are simultaneously valid corresponds to temperatures between (278 and 473) K and pressures up to 202 MPa. In comparison, the two agree to within ±0.12% at $P \geq 50$ MPa for all temperatures within that range. However, at lower pressures and $T \geq 400$ K, the correlation of Mylona et al.[28] shows positive deviations from the present model, reaching approximately 0.4% at $T = 473$ K. Mylona et al.[28] report two independent correlations for viscosity and the comments below apply only on their modified Vogel-Fulcher-Tammann equation, in which temperature and pressure are the independent variables. This correlation is valid at temperatures between (278 and 473) K and at pressures up to 200 MPa. Comparing that correlation with the present model first along the isobar at $P = 0.1$ MPa, a close agreement within ±2% over the entire temperature range was found. For higher pressures up to 100 MPa, agreement to within ±3% at temperatures up to approximately 450 K was found. However, at higher temperatures and higher pressures and the two models show significant differences that, at $P = 200$ MPa, span a range from -12% to 3%. Overall, based on the data sets deemed acceptable in this work by the regression analysis, the models presented by Mylona et al.[28] match the density data to within 0.05% (maximum APD 0.75%) and the viscosity data to 2.1% (maximum APD 54%) compared with 0.04% (maximum APD 0.14%) and 1.4% (maximum APD 4.9%) obtained from the present models. The pressure and temperature limits of the Mylona et al.[28] models are smaller than that of the present work (and was used outside the recommended limits) which could explain the large maximum APD difference between the two models on the accepted data sets.

12. CONCLUSIONS

Squalane has been identified as a preliminary viscosity standard for HTHP conditions. As a pure fluid of moderate viscosity it fills the gap between existing reference fluids until other HTHP reference fluids with higher viscosities have been evaluated. All the published data were reviewed and significant regions were identified where additional data were needed to fill voids, resolve discrepancies of existing data sets and to extend regions where the viscosity may be insufficiently modelled with the current techniques. New experimental measurements were performed to expand the data set in the areas of interest for high-temperature and high-pressure conditions. There appears to be some inconsistencies with the high pressure viscosity data (P > 400 MPa) and the low pressure data and/or the models used.

A large amount of empirical density and viscosity data was analysed to obtain new reference density and viscosity models for squalane. This was done using a novel approach to non-linear regression that combines global optimization and outlier detection algorithms. The resulting parameters are

substantially improved since they are not influenced by a small number of data points that deviate significantly from the bulk of the points.

This regression approach resulted in models which could reproduce the majority of the experimental density data to within an average of 0.04 % for density and 1.4 % for the viscosity data. Based on the data set used in the model regression (without outliers), the density model is limited to the pressure and temperature ranges of (0.1 to 202.1) MPa and (273 to 525) K, respectively. In addition, the viscosity model is limited to the pressure and temperature ranges of (0.1 to 467.0) MPa and (273 to 473) K. The maximum APD is 0.14% for density and 4.9% for viscosity. These models can be used to calibrate laboratory densitometers and viscometers at relevant HTHP conditions.

REFERENCES

(1) Tsujimoto, M. A Highly Unsaturated Hydrocarbon in Shark Liver Oil. *J. Ind. Eng. Chem*. **1916**, *8*, 889-896.

(2) Chapman, A. C. VIII.—Spinacene: A New Hydrocarbon from Certain Fish Liver Oil. *J. Chem. Soc., Trans.* **1917**, *111*, 56-69.

(3) Chapman, A. C. XC.—Spinacene: Its Oxidation and Decomposition *J. Chem. Soc. Trans.* **1923**, *123*, 769-779.

(4) Heilbron, I. M.; Hilditch, T. P.; Kamm, E. D. CCCCXX.—The Unsaponifiable Matter from the Oils of Elasmobranch Fish. Part II. The Hydrogenation of Squalene in the Presence of Nickel. *J. Chem. Soc.* **1926**, *129*, 3131-3136.

(5) Tsujimoto, M. Ueber das Hydrierte Squale. *Chem. Umsch. Geb. Fette, Oele, Wachse Harze* **1927**, *34*, 256-258.

(6) Sörensen, N. A.; Gillebo, T.; Holtermann, H.; Sörensen, J. S. Studies Related to Pristine VI. Synthesis of Digeranyl with some Remarks on the Physical Constants of Crocetane. *Acta. Chem. Scand.* **1951**, *5*, 757-765.

(7) Sax, K. J.; Stross, F. H. Squalane: A Standard. *Anal. Chem.* **1957**, *29*, 1700-1702.

(8) Whitmore, F. C.; Schiessler, R. W.; Dixon, J. A. *Properties of High Molecular Weight Hydrocarbons Synthesized by the Research Project 42 of the American Petroleum Institute*; American Petroleum Institute, New York, 1966.

(9) Cadogan, D. F.; Purnell, J. H. The Measurement of Organic Complex Formation Constants by Gas-Liquid Chromatography. *J. Chem. Soc. A* **1968**, 2133-2137.

(10) Cadogan, D. F.; Conder, J. R.; Locke, D. C.; Purnell, J. H. Concurrent Solution and Adsorption Phenomena in Chromatography. II. System Alcohols-Squalane. *J. Phys. Chem.* **1969**, *73*, 708-712.

(11) Kuss, E.; Taslimi, M. p,V,T-Messungen an zwanzig organischen Flüssigkeiten. *Chem. Ing. Tech*. **1970**, *42*, 1073–1081.

(12) Laub, R. J.; Purnell, J. H. Solvation of Complexing Studies. III. Further Evidence for a Microscopic Partitioning Theory of Solution. *J. Am. Chem. Soc.* **1976**, *98*, 30-35.

(13) Körösi, G.; Kováts, E. S. Density and surface tension of 83 organic liquids. *J. Chem. Eng. Data* **1981**, *26*, 323–332.

(14) Trejo, L. M.; Costas, M.; Patterson, D. Int. DATA Ser., Sel. Data Mixtures, Ser. A, 1991, (1), 12.

(15) Graaf, G. H.; Smit, H. J.; Stamhuis, E. J.; Beenackers, A. A. C. M. Gas-Liquid Solubilities of the Methanol Synthesis Components in Various Solvents. *J. Chem. Eng. Data* **1992**, *37*, 146-158.

(16) Kumagai, A.; Takahashi, S. Viscosity and Density of Liquid Mixtures of n-Alkanes with Squalane. *Int. J. Thermophys*. **1995**, 16, 773-779.

(17) Fermeglia, M.; Torriano, G. Density, Viscosity, and Refractive Index for Binary Systems of n-C16 and Four Nonlinear Alkanes at 298.15 K *J. Chem. Eng. Data* **2000**, 44, 965-969.

(18) Lal, K.; Tripathi, N.; Dubey, G. P. Densities, Viscosities, and Refractive Indices of Binary Liquid Mixtures of Hexane, Decane, Hexadecane, and Squalane with Benzene at 298.15 K. *J. Chem. Eng. Data* **2000**, *45*, 961-964.

(19) Fandiño, O.; Pensado, A. S.; Lugo, L.; Comuñas, M. J. P.; Fernández, J. Compressed Liquid Densities of Squalane and Pentaerythritol Tetra(2-ethylhexanoate). *J. Chem. Eng. Data* **2005**, *50*, 939-946.

(20) Fandiño, O.; Pensado, A. S.; Lugo, L.; Comuñas, M. J. P.; Fernández, J. Compressed Liquid Densities of Squalane and Pentaerythritol Tetra(2-ethylhexanoate). *J. Chem. Eng. Data* **2006**, *51*, 2274.

(21) Tripathi, N. Densities, Viscosities, and Refractive Indices of Mixtures of Hexane with Cyclohexane, Decane, Hexadecane, and Squalane at 298.15 K. *Int. J. Thermophys*. **2005**, *26*, 693-703.

(22) Kumagai, A.; Tomida, D.; Yokoyama C. Measurements of the Liquid Viscosities of Mixtures of n-Butane, n-Hexane, and n-Octane with Squalane to 30 MPa. *Int. J. Thermophys*. **2006**, *27*, 376-393.

(23) Tomida, D.; Kumagai, A.; Yokoyama C. Viscosity Measurements and Correlation of the Squalane + CO_2 Mixture. *Int. J. Thermophys*. **2007**, 28, 133-145.

(24) Dubey, G. P.; Sharma, M. Excess Volumes, Densities, Speeds of Sound, and Viscosities for the Binary Systems of 1-Octanol with Hexadecane and Squalane at (298.15, 303.15 and 308.15) K. *Int. J. Thermophys*. **2008**, 29, 1361-1375.

(25) Harris, K. R.; Temperature and Pressure Dependence of the Viscosities of 2-Ethylhexyl Benzoate, Bis(2-ethylhexyl) Phthalate, 2,6,10,15,19,23-Hexamethyltetracosane (Squalane), and Diisodecyl Phthalate. *J. Chem. Eng. Data*, **2009**, *54*, 2729–2738.

(26) Ciotta, F.; Maitland, G.; Smietana, M.; Trusler, J. P. M.; Vesovic, V. Viscosity and Density of Carbon Dioxide + 2, 6, 10, 15, 19, 23-Hexamethyltetracosane (Squalane). *J. Chem. Eng. Data* **2009**, *54*, 2436-2443.

(27) Fandiño, O.; Lugo, L.; Comuñas, M.J.P.; López, E.R.; Fernández, J. Temperature and pressure dependences of volumetric properties of two poly(propylene glycol) dimethyl ether lubricants. *J. Chem. Thermodyn.* **2010**, *42*, 84-89.

(28) Mylona, S.K.; Assael, M.J.; Comuñas, M.J.P.; Paredes, X.; Gaciño, F.M.; Fernández, J.; Bazile, J.P.; Boned, C.; Daridon, J.L.; Galliero, G.; Pauly, J.; Harris, K.R. Reference Correlations for the Density and Viscosity of Squalane from 273 to 473 K at Pressures to 200 MPa. *J. Phys. Chem. Ref. Data* **2014**, *43*, 013104.

(29) Sax, K. J.; Stross, F. H. Synthesis of Squalane. *J. Org. Chem*. **1957**, *22*, 1251-1252.

(30) Kuss, E.; Golly, H. Das Viskositäts Druckverhalten von Gas-Flüssigkeitslösungen. *Ber. Bunsenges Phys. Chem.* **1972***, 76*, 131-138.

(31) Barlow, A. J.; Erginsav, A. Viscoelastic Retardation of Supercooled Liquids. *Proc. R. Soc. Lond. A* **1972**, *327*, 175-190.

(32) Ratkovics, F.; Salamon, T.; Domonkos, L. Properties of Alcohol-Amine Mixtures, VI A Method for the Determoination of the Average Degree of Association. *Acta. Chim. Acad. Sci. Hungar.* **1974**, *83*, 71-77.

(33) Jambon, C.; Delmas, G. Viscosities of Mixtures of SnR_4 Compounds and of Some other Large Globular Molecules. Effect of Size Difference. *Can. J. Chem.* **1977**, *55*, 1360-1366.

(34) Glowinkowski, S.; Gisser, D. J.; Ediger, M. D.; Carbon-13 Nuclear Magnetic Resonance Measurements of Local Segmental Dynamics of Polyisoprene in Dilute Solution: Nonlinear Viscosity Dependence. *Macromolecules (Washington, DC, U. S.)*, **1990**, *23*, 3520–3530.

(35) Krahn, U. G.; Luft, G. Viscosity of Several Liquid Hydrocarbons in the Temperature Range 298-453 K at Pressures up to 200 MPa. *J. Chem. Eng. Data* **1994**, *39*, 670–672.

(36) Bair, S. The High Pressure Rheology of Some Simple Model Hydrocarbons. *Proc. Instn. Engrs.* **2002**, *216*, 139-149.

(37) Bair, S.; McCabe, C.; Cummings, P. T.; Calculation of Viscous EHL Traction for Squalane using Molecular Simulation and Rheometry. *Tribology Lett*. **2002**, *13*, 251-254.

(38) Pensado, A. S.; Comuñas, M. J. P.; Lugo, L. Fernández, J. High-Pressure Characterization of Dynamic Viscosity and Derived Properties for Squalane and Two Pentaerythritol Ester Lubricants: Pentaerythritol Tetra-2-ethylhexanoate and Pentaerythritol Tetranonanoate. *Ind. Eng. Chem. Res.* **2006**, *45*, 2394-2404.

(39) Bair, S. Reference Liquids for Quantitative Elastohydrodynamics: Selection and Rheological Characterization. *Tribology Lett*. **2006**, *22*, 197-206.

(40) Paredes, X.; Fandiño, O.; Comuñas, M. J. P.; Pensado, A. S.; Fernández, J. Study of the Effects of Pressure on the Viscosity and Density of Diisodecyl Phthalate. *J. Chem. Thermo.* **2009**, *41*, 1007-1015.

(41) Comuñas, M.J.P.; Paredes, X.; Gaciño, F.M.; Fernández, J.; Bazile, J.P.; Boned, C.; Daridon, J.L.; Galliero, G.; Pauly, J.; Harris, K.R.; Assael, M.J.; Mylona, S.K. Reference Correlation of the Viscosity of Squalane from 273 to 373 K at 0.1 MPa. *J. Phys. Chem. Ref. Data* **2013**, 42, 033101.

(42) Comuñas, M.J.P.; Paredes, X.; Gaciño, F.M.; Fernández, J.; Bazile, J.P.; Boned, C.; Daridon, J.L.; Galliero, G.; Pauly, J.; Harris, K.R. Viscosity measurements for squalane at high pressures to 350 MPa from T = (293.15 to 363.15)K. *J. Chem. Thermodyn.* **2014**, 69, 201-208.

(43) Viskrebentsev, V.; Petrova, A.; Ganieva, L. The Research about Isoprenoid Hydrocarbons as Viscous Components. *Izv. Vyssh. Uchebn. Zaved., Neft Gaz* **1978**, *21*, 64-65.

(44) Dilchert, G.; Kuss, E. The Experimental Determination of Gas Solubility in Mineral-Oils and the Viscosity-Pressure Behavior of the Gas/Oil Solution Up to 1 kbar. SPE 9025-MS **1980**.

(45) Kuss, E.; Dilchert, G. The Influence of Dissolved Gases on the Viscosity of Gas/Oil-Solutions at High Pressure. SPE 10534-MS **1981**.

(46) Kuss, E. The Viscosity of Gas/Oil Solutions at High Pressure, *High Temp. - High Pressures* **1983**, *15*, 93-105.

(47) Kuss, E.; Killesreiter, H. Sekundärförderung: Änderung der Viskosität und Kompressibilität von Mineralölen durch gelöstes Gas. BMFT-FB T 81-225, Forschungsbericht / Bundesministerium für Forschung und Technologie : Technolog. Forschung u. Entwicklung, **1981**.

(48) Deegan, R.D.; Leheny, R. L.; Menon, N.; Nagel, S. R. Dynamic Shear Modulus of Tricresyl Phosphate and Squalane. *J. Phys. Chem. B*, **1999**, *103*, 4066-4070.

(49) Roland, C. M.; Bair, S.; Casalini, R. Thermodynamic Scaling of the Viscosity of van der Waals, H-bonded, and Ionic Liquids. *J. Chem. Phys.* **2006**, *125*, 124508.

(50) Ling, G. H.; Shaw, M. T. Reversible Thermal Gelation of Soft Semi-Crystalline Polyethylene Microparticles With Surface Interactions in Squalane. *Polymer Egn. Sci.* **2008**, *48*, 329-335.

(51) Sautermeister, F. A.; Priest, M. Physical and Chemical Impact of Sulphuric Acid on Cylinder Lubrication for Large 2-Stroke Marine Diesel Engines. *Tribol. Lett.* **2012**, *47*, 261-271.

(52) Hata, H.; Tamoto, Y. High-Pressure Viscosity Measurements for Various Lubricants, and Prediction of Atmospheric Pressure-Viscosity Coefficient from the Easily Measurable Properties of Lubricant (Part 1) - Results of Mineral Oils. *J. Jpn. Soc. Tribol. (Toraiborojisuto)* **2010**, *55*, 635-646.

(53) Bhatia, S. C.; Tripathi, N.; Dubey, G. P. Density and Viscosity of Ternary Liquid Mixtures of Squalane with (Hexane+Benzene), (Cyclohexane+Benzene) and (Hexane+Cyclohexane) at 298.15 K. *Indian J. Chem.* **2003**, *42A*, 2513-2517.

(54) Bhatia, S. C.; Tripathi, N.; Dubey, G. P. Refractive Indices of Binary Liquid Mixtures of Squalane with Benzene, Cyclohexane and Hexane at 298.15 to 313.15 K. *Indian J. Pure App. Phys.* **2001**, *39*, 776-780.

(55) Dubey, G. P.; Sharma, M. Temperature and Composition Dependence of the Densities, Viscosities, and Speeds of Sound of Binary Liquid Mixtures of 1-Butanol with Hexadecane and Squalane. *J. Chem. Eng. Data* **2008**, *53*, 1032-1038.

(56) Dubey, G. P.; Sharma, M. Thermodynamic and Transport Behavior of Binary Liquid Mixtures of 1-Decanol with Hexadecane and Squalane at 298.15, 303.15 and 308.15 K. *Z. Phys. Chem.* **2008**, *222*, 1065-1082.

(57) Dubey, G. P.; Sharma, M.; Oswal, S. Volumetric, Transport, and Acoustic Properties of Binary Mixtures of 2-methyl-1-Propanol with Hexadecane and Squalane at T = (298.15, 303.15, and 308.15) K: Experimental Results, Correlation, and Prediction by the ERAS model. *J. Chem. Thermo.* **2009**, *41*, 849-858.

(58) Dubey, G. P.; Sharma, M. Studies of Mixing Properties of Binary Systems of 2-Propanol with Hexadecane and Squalane at T= (298.15, 303.15, and 308.15) K. *J. Chem. Thermo.* **2009**, *41*, 115-122.

(59) Dubey, G. P.; Sharma, M. Thermodynamic and Transport Properties of Binary Liquid Mixtures of 1-Hexanol with Hexadecane and Squalane at 298.15, 303.15 and 308.15 K. *Z. Phys. Chem.* **2009**, *223*, 279-298.

(60) Denis, J. The Relationships Between Structure and Rheological Properties of Hydrocarbons and Oxygenated Compounds used as Base Stocks. *J. Syn. Lub.* **1984**, *1*, 201-238.

(61) Sheridan, J. P.; Capeless, M. A.; Martire, D. E. Thermodynamics of Molecular Association by Gas-Liquid Chromatography. III. Aromatic Compounds with Tetra-n-butyl Pyromellitate. *J. Am. Chem. Soc.* **1972**, *94*, 3298-3302.

(62) Kumagai, A.; Tomida, D.; Yokoyama C. Measurements of the Liquid Viscosities of Mixtures of Isobutane with Squalane to 30 MPa. *Int. J. Thermophys.* **2007**, *28*, 1111-1119.

(63) Schmidt, K. A. G.; Quiñones-Cisneros, S. E.; Carroll, J. J.; Kvamme, B. Hydrogen Sulfide Viscosity Modeling. *Energy Fuels* **2008**, *22*, 3424-3434.

(64) Quiñones-Cisneros, S. E.; Schmidt, K. A. G.; Binod, R.G.; Blais, P.; Marriott, R. A. Reference Correlation for the Viscosity Surface of Hydrogen Sulfide *J. Chem. Eng. Data* **2012**, *57*, 3014–3018.

(65) Mondello, M.; Grest, G. S. Viscosity Calculations of n-Alkanes by Equilibrium Molecular Dynamics. *J. Chem. Phys.* **1997**, *106*, 9327-9336.

(66) Moore, J. D.; Cui, S. T.; Cochran, H. D.; Cummings, P. T. Lubricant Characterization by Molecular Simulation. *AIChE J.* **1997**, *43*, 3260-3263.

(67) Gupta, S. A.; Cochran, H. D.; Cummings, P. T. Shear Behavior of Squalane and Tetracosane under Extreme Confinement. III. Effect of Confinement on Viscosity. *J. Chem. Phys.* **1997**, *107*, 10335-10343.

(68) Cui, S. T.; Cummings, P. T.; Cochran, H. D.; Moore, J. D.; Gupta, S. A. Configurational Bias Gibbs Ensemble Monte Carlo Simulation of Vapor-Liquid Equilibria of Linear and Short-Branched Alkanes. *Fluid Phase Equilib*. **1997**, 141, 45-61.

(69) Cui, S. T.; Cummings, P. T.; Cochran, H. D. Nonequilibrium Molecular Dynamics Simulation of the Rheology of Linear and Branched Alkanes. *Int. J. Thermophys*. **1998**, *19*, 449-459.

(70) Neubauer, B.; Delhommelle, J.; Boutin, A.; Tavitian, B.; Fuchs, A. H. Monte Carlo Simulations of Squalane in the Gibbs Ensemble. *Fluid Phase Equilib.* **1999**, *155*, 167-176.

(71) Moore, J. D.; Cui, S. T.; Cochran, H. D.; Cummings, P. T. Rheology of Lubricant Basestocks: A Molecular Dynamics Study of C_{30} Isomers. *J. Chem. Phys.* **2000**, *113*, 8833-8840.

(72) McCabe, C.; Cui, S.; Cummings, P. T. Characterizing the Viscosity–Temperature Dependence of Lubricants by Molecular Simulation. *Fluid Phase Equilib.* **2001**, *183-184*, 363-370.

(73) Liu Y.; Wang, Q. J.; Wang, W.; Hu, Y.; Zhu, D.; Krupka, I.; Hartl, M. EHL Simulation using the Free-Volume Viscosity Model. *Tribology Lett.* **2006**, *23*, 27-37.

(74) Caudwell, D.R.; Trusler, J.P.M.; Vesovic, V.; Wakeham, W.A. The viscosity and density of n-dodecane and n-octadecane at pressures up to 200 MPa and temperatures up to 473 K. *Int. J. Thermophys.* **2004**, *25*, 1339-1352.

(75) Caudwell, D.R.; Trusler, J.P.M.; Vesovic, V.; Wakeham, W.A. Viscosity and Density of Five Hydrocarbon Liquids at Pressures up to 200 MPa and Temperatures up to 473 K. *J. Chem. Eng. Data* **2009**, *54*, 359-366.

(76) Ciotta, F., Viscosity of Asymmetric Liquid Mixtures Under Extreme Conditions, in Chemical Engineering. **2010**, Imperial College London: London. 260.

(77) Retsina, T.; Richardson, S.M.; Wakeham, W.A. The Theory of a Vibrating-Rod Viscometer. *Appl. Sci. Res.* **1987**, *43*, 325-346.

(78) Retsina, T.; Richardson, S.M.; Wakeham, W.A. The Theory of a Vibrating-Rod Densimeter. *Appl. Sci. Res.* **1986**, *43*, 127-158.

(79) Audonnet, F.; Pádua, A.A.H. Simultaneous measurement of density and viscosity of n-pentane from 298 to 383 K and up to 100 MPa using a vibrating-wire instrument. *Fluid Phase Equilib.* **2001**, *181*, 147-161.

(80) Ciotta, F.; Trusler, J.P.M. Improved Understanding of Vibrating-Wire Viscometer-Densimeters. *J. Chem. Eng. Data* **2010**, *55*, 2195-2201.

(81) Dymond, J. H.; Malhotra, R. The Tait Equation: 100 Years On. *Int. J. Thermophys*. **1988**, *9*, 941–951.

(82) Comuñas, M. J. P.; Baylaucq, A.; Boned, C.; Fernández, J. High-Pressure Measurements of the Viscosity and Density of Two Polyethers and Two Dialkyl Carbonates. *Int. J. Thermophys*. **2001**, *22*, 750-768.

(83) Whittaker, E.T.; Robinson, G. *The Calculus of Observations: An Introduction to Numerical Analysis*; Dover Publications, New York, 1924.

(84) Benjamini, Y.; Hochberg, Y. Controlling the False Discovery Rate: A Practical and Powerful Approach to Multiple Testing; *J. R. Stat. Soc. B* **1995**, *57*, 289-300.

(85) Weiland, R.H.; Chakravarty, T.; Mather, A.E. Solubility of Carbon Dioxide and Hydrogen Sulfide in Aqueous Alkanolamines. *Ind. Eng. Chem*. *Res.* **1993**, *32*, 1419-1430.

(86) Price, K.; Storn, R.; Lampinen, J. *Differential Evolution - A Practical Approach to Global Optimization*, Springer-Verlag, Berlin Heidelberg, Germany, 2005.

Table 1. Summary of the available literature data for the density of squalane

Investigators	Year	# of Points	*T*/K	*P*/MPa	Method	Purity	Stated Accuracy	Reference
Tsujimoto	1916	1	288.15	0.1	NR	$n_D^{20^\circ}$=1.4525	NR	1
Chapman	1917	1	293.15	0.1	NR	$n_D^{20^\circ}$=1.4547	NR	2
Chapman	1923	2	288.15-293.15	0.1	NR	$n_D^{20^\circ}$=1.4532	NR	3
Heilbron et al.	1926	1	293.15	0.1	NR	$n_D^{20^\circ}$=1.4534	NR	4
Tsujimoto	1927	2	288.15-293.15	0.1	NR	$n_D^{20^\circ}$=1.4515	NR	5
Sörensen et al.	1951	4	293.15	0.1	NR	$n_D^{20^\circ}$=1.4528	NR	6
Sax and Stross	1957	1	293.15	0.1	NR	$n_D^{20^\circ}$=1.4516	0.004%	7
Whitmore et al.	1966	5	273.15-372.05	0.1	NR	$n_D^{20^\circ}$=1.4522	NR	8
Cadogan and Purnell	1969	3	323.15-343.15	0.1	Dilatometry	~99%	NR	9
Cadogan et al.	1969	1	353.15	0.1	Pyknometry	~99%	NR	10
Kuss and Taslimi	1970	24	297.99-352.98	0.1-196	Dilatometry	NR	NR	11
Laub and Purnell	1976	3	329.15-373.15	0.1	Dilatometry	NR	0.10%	12
Kőrösi and Kováts	1981	4	293.15-473.15	0.1	Pycnometer	$n_D^{20^\circ}$=1.4521	0.05%	13
Trejo et al.	1991	1	298.15	0.1	Vibrating Tube Densimeter	99 mol%	0.06%	14
Graaf et al.	1992	14	293.2-561.6	0.1	Gravimetric	99%	0.50%	15
Kumagai and Takahashi	1995	5	298.15	0.1	Glass Pycnometer	>99%	0.04%	16
Fermeglia and Torriano	1999	1	298.15	0.1	Vibrating Tube Densimeter	99%	0.001%	17
Lal et al.	2000	1	298.15	0.1	Bicapillary Pycnometer	$n_D^{25^\circ}$=1.4474	0.70%	18
Fandiño et al.	2005	99	278.15-353.15	0.1-45	Vibrating Tube Densimeter	99%	0.06%	19,20
Tripathi	2005	1	298.15	0.1	Bicapillary Pycnometer	$n_D^{25^\circ}$=1.4474	0.70%	21
Kumagai et al.	2006	16	273.15-333.15	0.1-30	Glass Piezometer	NR	0.40%	22
Tomida et al.	2007	12	293.15-353.15	0.1-30	Glass Piezometer	98%	0.40%	23
Dubey and Sharma	2008	3	298.15-308.15	0.1	Vibrating Tube Densimeter	>99%	0.002%	24
Harris	2009	12	273.15-363.15	0.1	Vibrating Tube Densimeter	>99%	0.50%	25
Ciotta et al.	2009	32	303.18-448.25	1.07-176.1	Vibrating Wire Apparatus	>99 wt%	0.20%	26
Fandiño et al.	2010	53	298.15-398.15	0.1-60	Vibrating Tube Densimeter*	99%*	0.7-1.0%*	27
Mylona et al.	2014	19	283.15-373.15	0.1	Vibrating Tube Densimeter	NR	NR	28
New data	2010	86	338.19-473.07	0.15-202.1	Vibrating Wire Apparatus	>99 wt%	0.20%	

NR = not reported

*As described by Mylona et al.[28]

Table 2. Summary of the available literature data for the viscosity of squalane

Investigators	Year	# of Points	*T*/K	*P*/MPa	Method	Purity	Stated Accuracy	Reference
Sax and Stross	1957	2	310.8-371.9	0.1	NR	$n_D^{20^o}$=1.4516	1%	7
Sax and Stross	1957	1	310.8	0.1	NR	$n_D^{20^o}$=1.4520	NR	29
Whitmore et al.	1966	10	273.2-372.1	0.1	NR	$n_D^{20^o}$=1.4522	NR	8
Kuss and Golly	1972	26	298.2-313.2	0.1-98.1	Falling Sinker		0.40%	30
Barlow and Erginsav	1972	10	242.7-311.3	0.1	Suspended level Viscometer - Capillary B.S. 188	NR	0.50%	31
Ratkovics et al.	1974	7	293-353	0.1	Höppler Rheoviscosimeter	NR	NR	32
Jambon and Delmas	1977	1	298.2	0.1	Ubbelohde Type	NR	0.20%	33
Glowinkowski et al.	1990	1	333	0.1	Cannon-Fenske Capillary Flow Viscometer	>99%	1%	34
Krahn and Luft	1994	18	298.2-453.2	0.1-195	Rolling Ball	99%	2%	35
Kumagai and Takahashi	1995	4	273.2-333.2	0.1	Capillary	>99%	1.70%	16
Fermeglia and Torriano	1999	1	298.2	0.1	Ubbelohde Type	99%	0.00%	17
Lal et al.	2000	1	298.2	0.1	Ubbelohde Type	$n_D^{25^o}$=1.4474	0.01%	18
Bair	2002	32	313.2-373.2	0.1-1298	Falling Body	99%	3%	36
Bair et al.	2002	6	303.2	0.1-378	Falling Body	99%	3%	37
Tripathi	2005	1	298.2	0.1	Ubbelohde Type	$n_D^{25^o}$=1.4474	0.90%	21
Pensado et al.	2006	84	303.2-353.2	0.1-60	Rolling Ball	>99 mol%	3%	38
Kumagai et al.	2006	12	293.2-333.2	0.1-30	Falling Body	NR	3%	22
Bair	2006	46	293.2-373.2	0.1-1200	Falling Body	99%	3%	39
Tomida et al.	2007	6	293.2-353.2	10-20	Rolling Ball	98%	3%	23
Dubey and Sharma	2008	3	298.2-308.2	0.101	Ubbelohde Type	>99%	0.01%	24
Paredes et al.	2009	84	303.2-353.2	0.1-60	Rolling Ball	NR	4%	40
Harris	2009	151	273.2-353.2	0.1-378.6	Falling Body	>99%	2%	25
Ciotta et al.	2009	32	303.2-448.3	1.07-176.1	Vibrating Wire	>99 wt%	2%	26
Comuñas et al.	2013	54	278.15-373.15	0.1	Various*	>99%	1-2%*	41
Comuñas et al.	2014	176	303.15-363.15	9.2-349.8	Various**	>99%	2.3-5%**	42
New data	2010	86	338.19-473.07	0.15-202.1	Vibrating Wire	>99 wt%	2%	

NR = not reported

*Falling Body (*2%*), Ubbelohde Capillary (< *1%*), Quartz-Crystal Resonator *(2%*), Rotating-Cylinder (*1%*), Vibrating Wire (*1%*)

**Falling Body (four different systems ranging 2.3% -5%), Quartz-Crystal Resonator (*4%)*

Table 3. Diameters *d* of the vibrating wire measured as a function of axial position and rotation

Axial position:	-20 mm	Centre	+20 mm
Angle	*d*/mm	*d*/mm	*d*/mm
0°	0.15101	0.15122	0.15121
36°	0.15102	0.15112	0.15121
72°	0.15101	0.15113	0.15124
108°	0.15099	0.15115	0.15119
144°	0.15097	0.15116	0.15113

Table 4. Purity of Squalane

Chemical Name	Source	Minimum Stated Purity/Mass Fraction%
Squalane[a]	Sigma Aldrich	0.99[b]

[a] $C_{30}H_{62}$; 2,6,10,15,19,23-hexamethyltetracosane [b] No purification was attempted

Table 5. Viscosities η and densities ρ of S20 measured in the vibrating-wire instrument at ambient pressure and temperatures T, and differences $\Delta\eta$ and $\Delta\rho$ from the values certified by the supplier.[a]

	Measured	Certified	Difference	Measured	Certified	Difference
T/K	η/mPa·s	η/mPa·s	$\Delta\eta/\eta$	ρ/kg·m^{-3}	ρ/kg·m^{-3}	$\Delta\rho/\rho$
298.15	29.48	29.23	0.8 %	857.3	859.4	-0.25 %
323.15	10.72	10.70	0.2 %	841.1	843.3	-0.26 %
353.15	4.624	4.619	0.1 %	821.4	824.0	-0.31 %

[a] standard uncertainties are $u(T) = 0.02$ K, $u(\eta) = 0.01 \cdot \eta$, and $u(\rho) = 0.001 \cdot \rho$

Table 6. Kinematic viscosity μ and density ρ measured at ambient pressure and temperature T and differences $\Delta\rho$ and $\Delta\eta$ between the densities and derived dynamic viscosities and those determined from the vibrating-wire measurements.[a]

Sample	T/K	μ/mm·s^{-1}	ρ/kg·m^{-3}	$\Delta\rho/\rho$	η/mPa·s	$\Delta\eta/\eta$
Fresh	338.38	8.665	779.71	0.12%	6.756	0.7 %
Used	338.22	8.583	779.53	0.08 %	6.691	-0.7 %

[a] standard uncertainties are $u(T) = 0.02$ K, $u(\mu) = 0.002 \cdot \mu$ and $u(\rho) = 0.0001 \cdot \rho$.

Table 7. Experimental viscosities η and densities ρ measured with the vibrating-wire instrument at temperatures T and pressures P.[a]

T/K	P/MPa	η/mPa·s	ρ/kg·m^{-3}	T/K	P/MPa	η/mPa·s	ρ/kg·m^{-3}
338.19	1.05	6.815	779.26	433.36	0.68	1.309	717.22
338.19	21.21	9.666	792.77	433.31	0.60	1.309	717.04
338.20	40.64	13.185	803.93	433.35	20.50	1.749	737.74
338.20	60.42	17.706	814.29	433.36	40.31	2.231	753.83
338.20	79.83	23.480	822.46	433.19	60.43	2.785	767.55
338.20	100.23	30.939	831.55	433.20	80.19	3.392	779.13
338.21	119.82	40.324	837.96	433.21	100.28	4.072	789.84
338.20	140.24	52.304	845.12	433.21	120.04	4.865	798.72
338.20	161.30	68.139	851.46	433.21	140.20	5.754	807.55
338.22	0.94	6.808	778.91	433.19	160.66	6.774	815.65
				433.19	180.70	7.891	823.09
373.12	0.78	3.125	756.09	433.19	200.37	9.057	830.05
373.12	20.35	4.234	771.55	433.18	1.12	1.324	717.80
373.12	39.97	5.565	784.50				
373.12	60.03	7.219	795.89	453.15	1.15	1.062	704.74
373.12	80.95	9.293	806.36	453.16	20.19	1.405	726.40
373.12	101.16	11.717	815.48	453.17	40.45	1.796	744.09
373.12	120.42	14.403	823.57	453.18	60.48	2.222	758.43
373.12	140.64	17.829	831.10	453.18	80.14	2.681	770.59
373.12	159.51	21.726	837.61	453.18	100.41	3.214	781.58
373.12	180.46	26.767	843.98	453.20	120.79	3.800	791.61
373.12	201.38	32.723	850.63	453.20	140.40	4.438	800.32
373.12	0.62	3.122	756.02	453.19	160.15	5.142	808.49
				453.20	180.71	5.945	816.55
388.14	1.10	2.436	746.78				
388.13	20.29	3.250	762.98	338.29 [b]	1.01	6.83	779.46
388.14	40.38	4.242	776.95				
388.14	59.85	5.392	788.53	452.95 [b]	163.17	5.261	809.30
388.13	80.49	6.828	799.25	452.95 [b]	180.27	5.937	815.84
388.13	101.53	8.548	809.12	452.85	201.77	6.867	823.37
388.13	120.96	10.458	817.16				
388.13	139.90	12.580	824.59	473.05	0.15	0.853	690.19
388.14	160.80	15.310	832.35	472.81	1.05	0.867	691.59
388.14	180.61	18.401	838.96	473.05	20.04	1.151	715.20
388.14	201.47	22.160	845.55	473.05	39.89	1.465	733.71
388.13	0.89	2.432	746.65	473.06	60.23	1.810	749.17
				473.06	79.91	2.175	761.86
413.17	1.05	1.691	730.56	473.07	100.37	2.590	773.42
413.18	20.11	2.233	748.65	473.05	120.20	3.031	783.48
413.18	40.28	2.885	763.94	473.05	140.44	3.531	792.71
413.18	60.20	3.620	776.68	473.05	160.34	4.073	801.00
413.21	80.74	4.485	788.16	473.05	180.47	4.671	808.83
413.22	100.35	5.454	797.82	473.03	200.21	5.348	815.83
413.22	120.46	6.574	806.56	473.04	1.05	0.868	691.45
413.24	140.20	7.831	815.07				
413.25	160.57	9.322	822.80				
413.25	181.45	11.116	829.85				
413.25	202.09	13.062	836.75				
413.24	0.61	1.680	730.10				

[a] standard uncertainties are $u(T)$ = 0.02 K, $u(p)$ = 0.02 MPa, $u(\eta)$ = 0.01·η, and $u(\rho)$ = 0.001·ρ

[b] Check measurements after adjustment of wire.

Table 8. Results of the regression analysis

Density

Parameter	Value
a_0 /kg·m^{-3}	9.789E+02
a_1 /kg·m^{-3}·K^{-1}	-5.355E-01
a_2 / kg·m^{-3}·K^{-2}	-1.571E-04
b_0 /MPa	2.000E-01
b_1 /MPa·K^{-1}	3.822E+02
b_2 / MPa·K^{-2}	-1.162E+00
C	9.305E-04

Regression Statistics

Number Points	407
Δ	0.04%
Bias	0.000%
Std. Dev.	0.05%
Max(Δ_i)	0.14%
T_{max}/K	524.70
T_{min}/K	273.15
P_{min}/MPa	0.098
P_{max}/MPa	202.09
Number Outliers	64

Viscosity

Parameter	Value
A_η /mPa·s	7.610E-02
B_η /K	7.528E+02
C_η /K	-1.707E+02
d_0	-4.488E+00
d_1 //K	3.330E+03
d_2 /K^2	1.736E+05
e_0 /MPa	-4.684E+02
e_1 /MPa·K^{-1}	5.072E+00
e_2 /MPa·K^{-2}	-7.421E-03

Regression Statistics

Number Points	853
Δ	1.4%
Bias	0.02%
Std. Dev.	1.8%
Max(Δ_i)	4.9%
T_{max}/K	473.07
T_{min}/K	242.70
P_{min}/MPa	0.098
P_{max}/MPa	467
Number Outliers	97

Table 9. Summary of regression results for the density of squalane

Investigators	Year	Reference	# of Points Used	# of Points Rejected	AAPD of Points Used (%)	AAPD of Points Rejected (%)
Tsujimoto	1916	1	1	0	0.12	--
Chapman	1917	2	0	1	--	0.89
Chapman	1923	3	0	2	--	0.26
Heilbron et al.	1926	4	1	0	0.10	--
Tsujimoto	1927	5	2	0	0.003	--
Sörensen et al.	1951	6	0	4	--	0.27
Sax and Stross	1957a	7	1	0	0.07	--
Whitemore et al.	1966	8	4	1	0.09	0.16
Cadogan and Purnell	1968	9	3	0	0.05	--
Cadogan et al.	1969	10	1	0	0.07	--
Kuss and Taslimi	1970	11	24	0	0.05	--
Laub and Purnell	1976	12	3	0	0.09	--
Kőrösi and Kováts	1981	13	3	1	0.06	0.39
Trejo et al.	1991	14	1	0	0.09	--
Graaf et al.	1992	15	5	9	0.08	0.43
Kumagai and Takahashi	1995	16	4	1	0.03	0.80
Fermeglia and Torriano	1999	17	1	0	0.02	--
Lal et al.	2000	18	1	0	0.02	--
Fandiño et al.	2005	19,20	99	0	0.02	--
Tripathi	2005	21	1	0	0.02	--
Kumagai et al.	2006	22	12	4	0.08	0.22
Tomida et al.	2007	23	1	11	0.06	0.35
Dubey and Sharma	2008	24	3	0	0.02	--
Harris	2009	25	12	0	0.04	--
Ciotta et al.	2009	26	12	20	0.07	0.36
Fandiño et al.	2010	27	53	0	0.04	--
Mylona et al.	2014	28	19	0	0.02	--
New Data	2010		77	9	0.04	0.19

Table 10. Summary of the regression results for the viscosity of squalane

Investigators	Year	Reference	# of Points Used	# of Points Rejected	AAPD of Points Used (%)	AAPD of Points Rejected (%)
Sax and Stross	1957a	7	2	0	0.83	--
Sax and Stross	1957b	29	1	0	2.02	--
Whitemore et al.	1966	8	5	3	1.05	28.49
Kuss and Golly	1972	30	26	0	1.06	--
Barlow and Erginsav	1972	31	9	1	4.10	15.45
Ratkovics et al.	1974	32	0	7	--	24.24
Jambon and Delmas	1977	33	1	0	3.33	--
Glowinkowski et al.	1990	34	1	0	1.73	--
Krahn and Luft	1994	35	5	13	2.02	9.86
Kumagai and Takahashi	1995	16	3	1	1.07	22.39
Fermeglia and Torriano	1999	17	1	0	1.12	--
Lal et al.	2000	18	0	1	--	10.23
Bair	2002	36	13	19	2.12	40.83
Bair et al.	2002	37	2	4	2.50	7.42
Tripathi	2005	21	0	1	--	10.23
Pensado et al.	2006	38	84	0	0.67	--
Kumagai et al.	2006	22	11	1	1.49	6.14
Bair	2006	39	15	31	2.64	40.22
Tomida et al.	2007	23	6	0	1.96	--
Dubey and Sharma	2008	24	3	0	1.55	--
Paredes et al.	2009	40	84	0	1.02	--
Harris	2009	25	150	1	1.23	5.22
Ciotta et al.	2009	26	31	1	2.40	5.53
Comuñas et al.	2013	41	54	0	0.72	--
Comuñas et al.	2014	42	170	6	1.49	7.20
New Data	2010		79	7	2.11	6.98

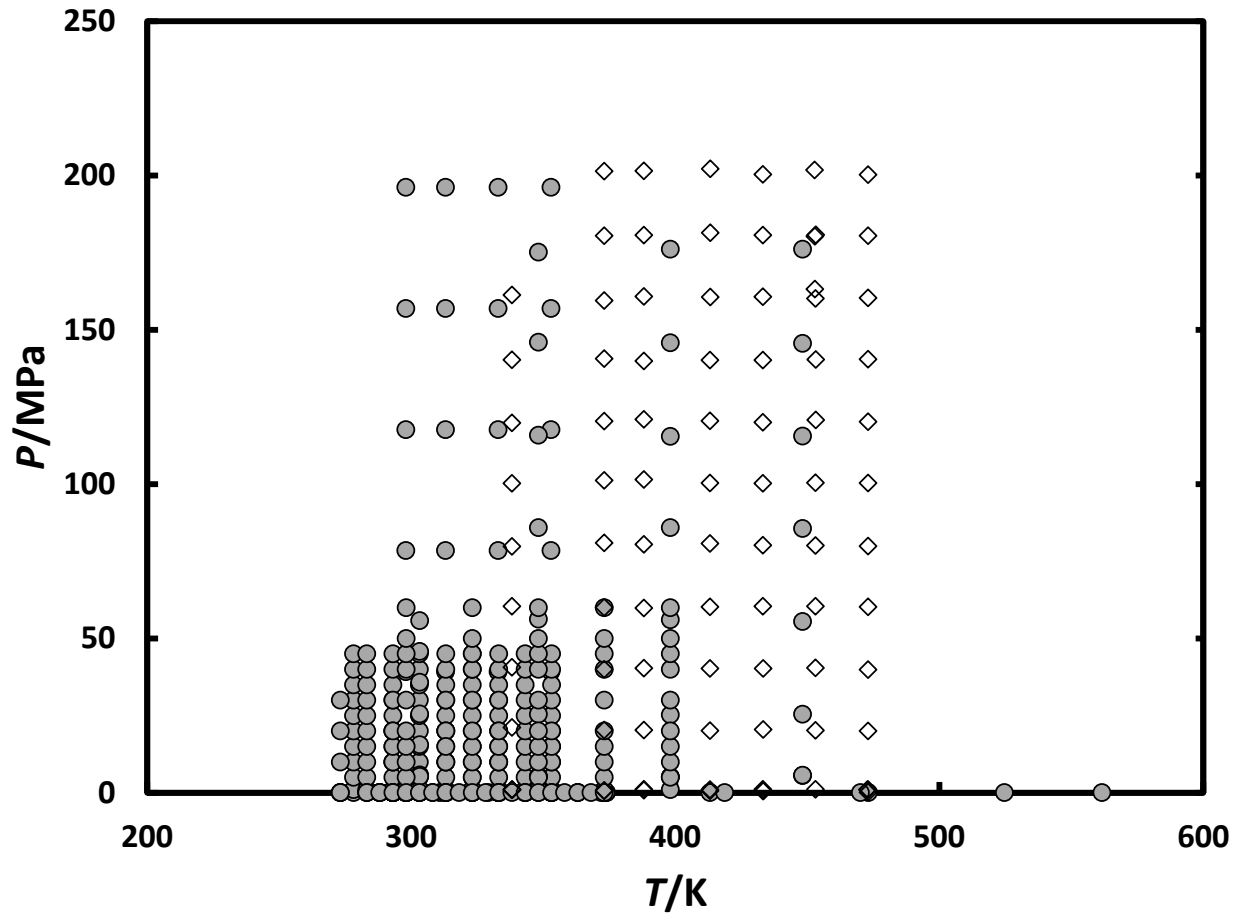

Figure 1. Pressure *P* and temperature *T* surface of the squalane experimental density investigations: ●, literature density data; ◇, new density data.

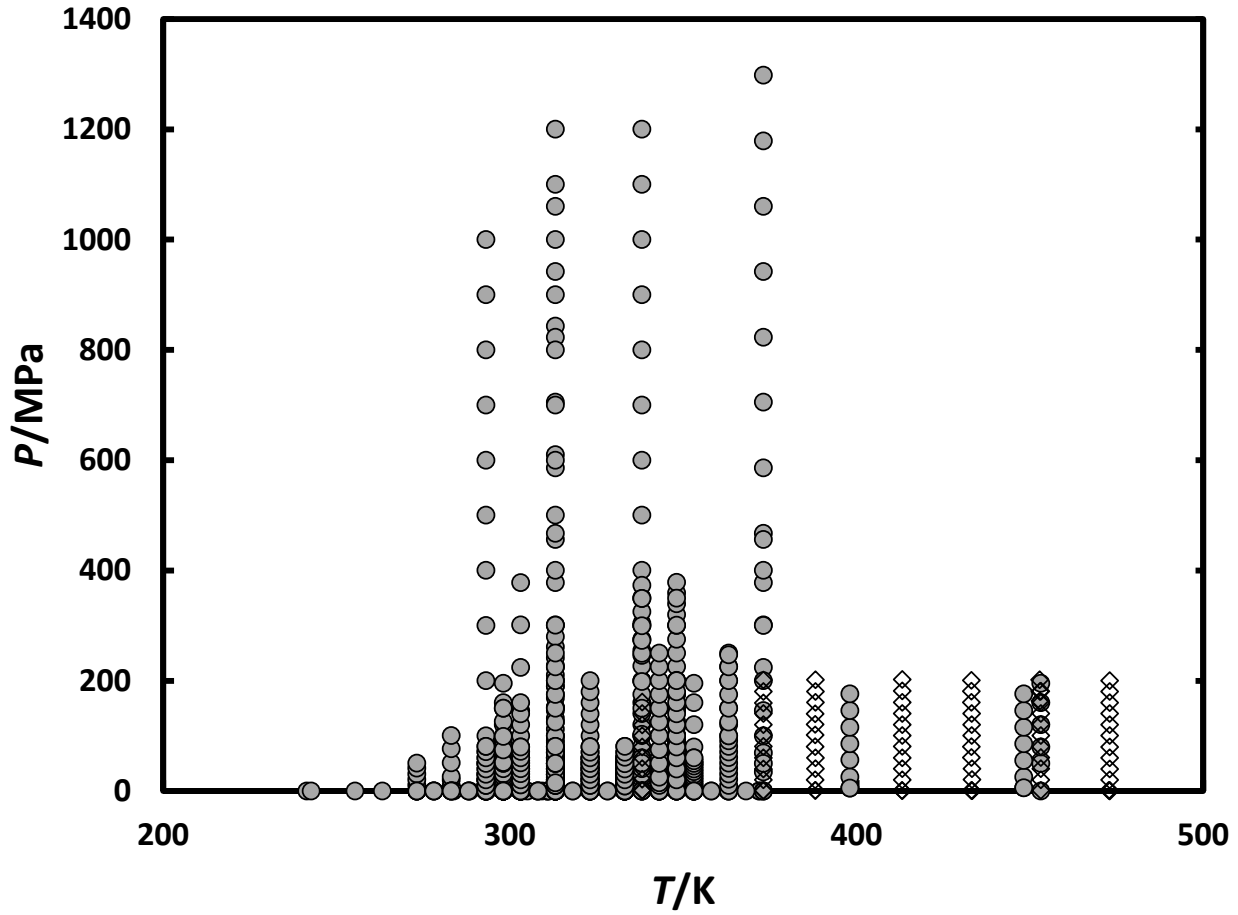

Figure 2. Pressure *P* and temperature *T* surface of the squalane experimental viscosity investigations: ●, literature density data; ◇, new density data.

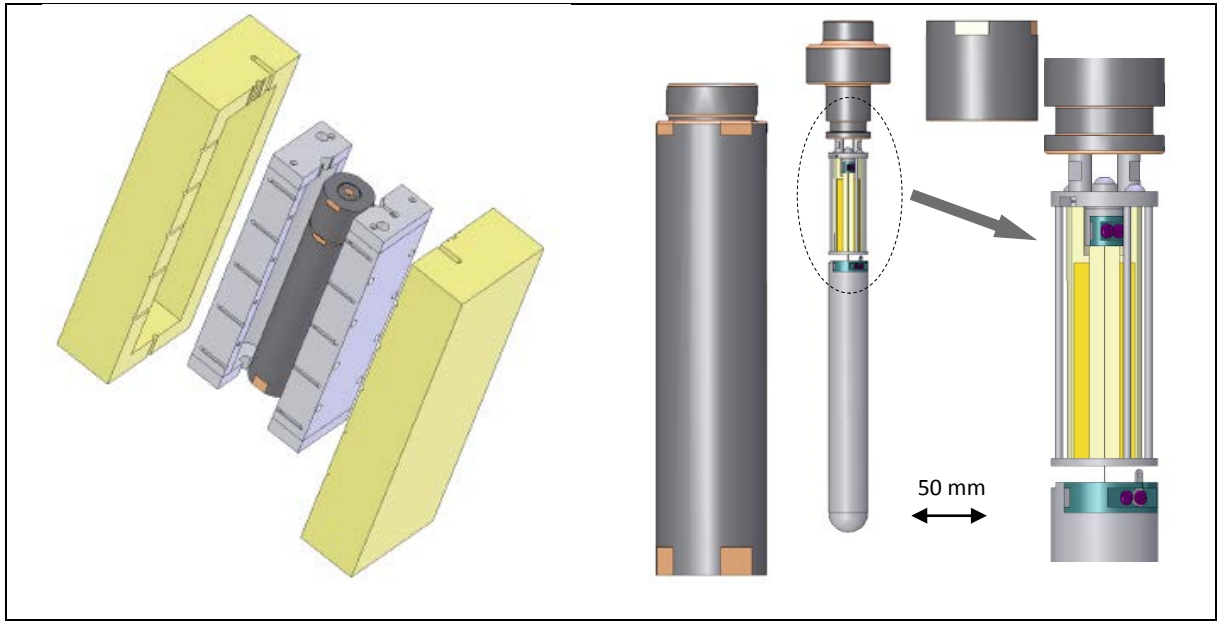

Figure 3. Visualisation of the vibrating-wire instrument. From the left: pressure vessel, aluminium block thermostat and outer insulation box; high-pressure vessel; plug closure, with sensor attached, and screw cap; details of the sensor showing the upper and lower wire clamps (green), magnets (gold) and the gold-plated soft-iron yoke (yellow).

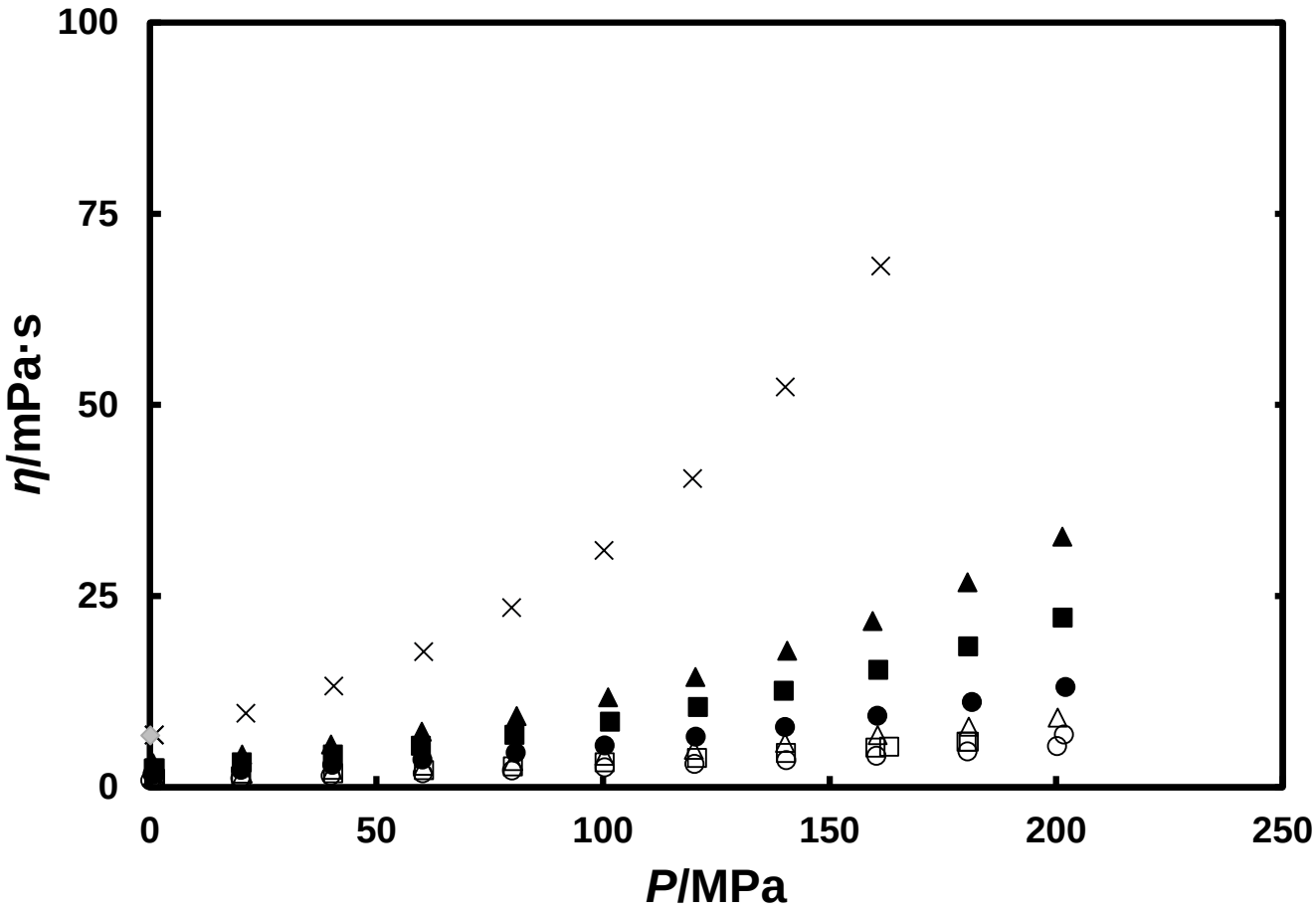

Figure 4. Viscosity η of squalane along seven isotherms as a function of pressure P: ×, T = 338 K; ▲, T = 373 K; ■, T = 388 K, ●, T = 413 K; △, T = 433 K; □, T = 453 K; ○, T = 473 K; ◆, capillary viscometer measurement at T = 338 K.

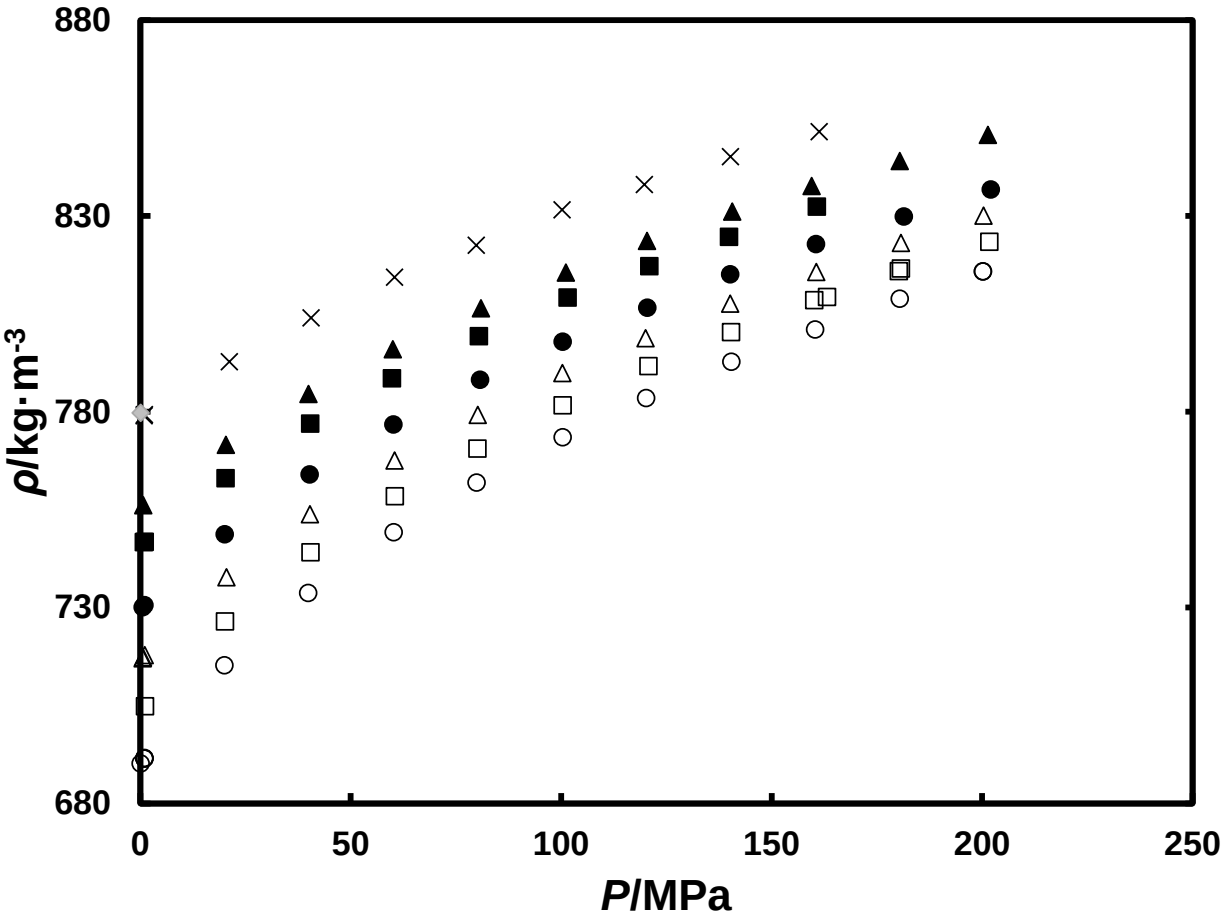

Figure 5. Density ρ of squalane along seven isotherms as a function of pressure P: ×, T = 338 K; ▲, T = 373 K; ■, T = 388 K, ●, T = 413 K; △, T = 433 K; □, T = 453 K; ○, T = 473 K; ◆, DMA 5000 vibrating-tube densimeter measurement at T = 338 K.

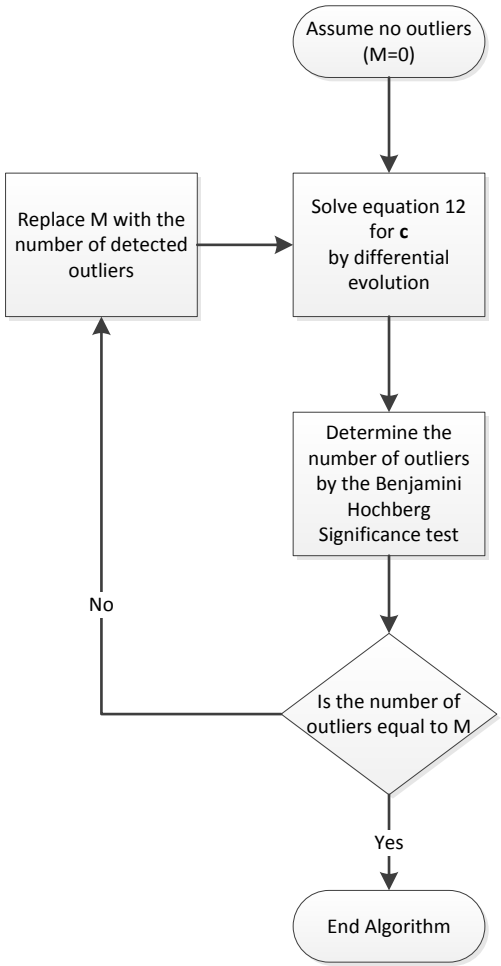

Figure 6. General algorithm of the robust regression routine.

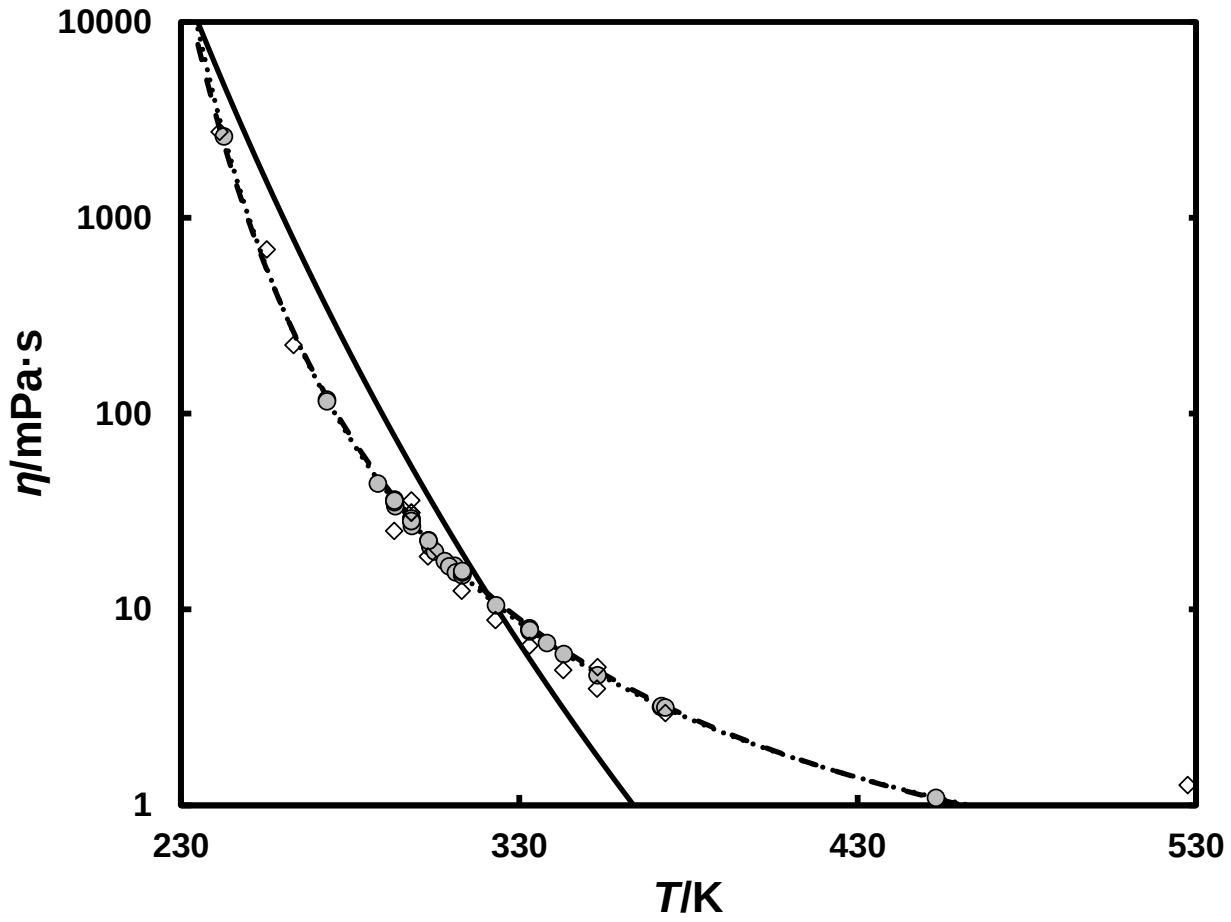

Figure 7. Comparison of regression methods for viscosity η at atmospheric pressure: solid line, least squares objective function (Equation 8); dashed line, relative objective function (Equation 10); dot line, robust regression with relative objective function (Equation 12); ●, literature data; ◇, literature data outliers.

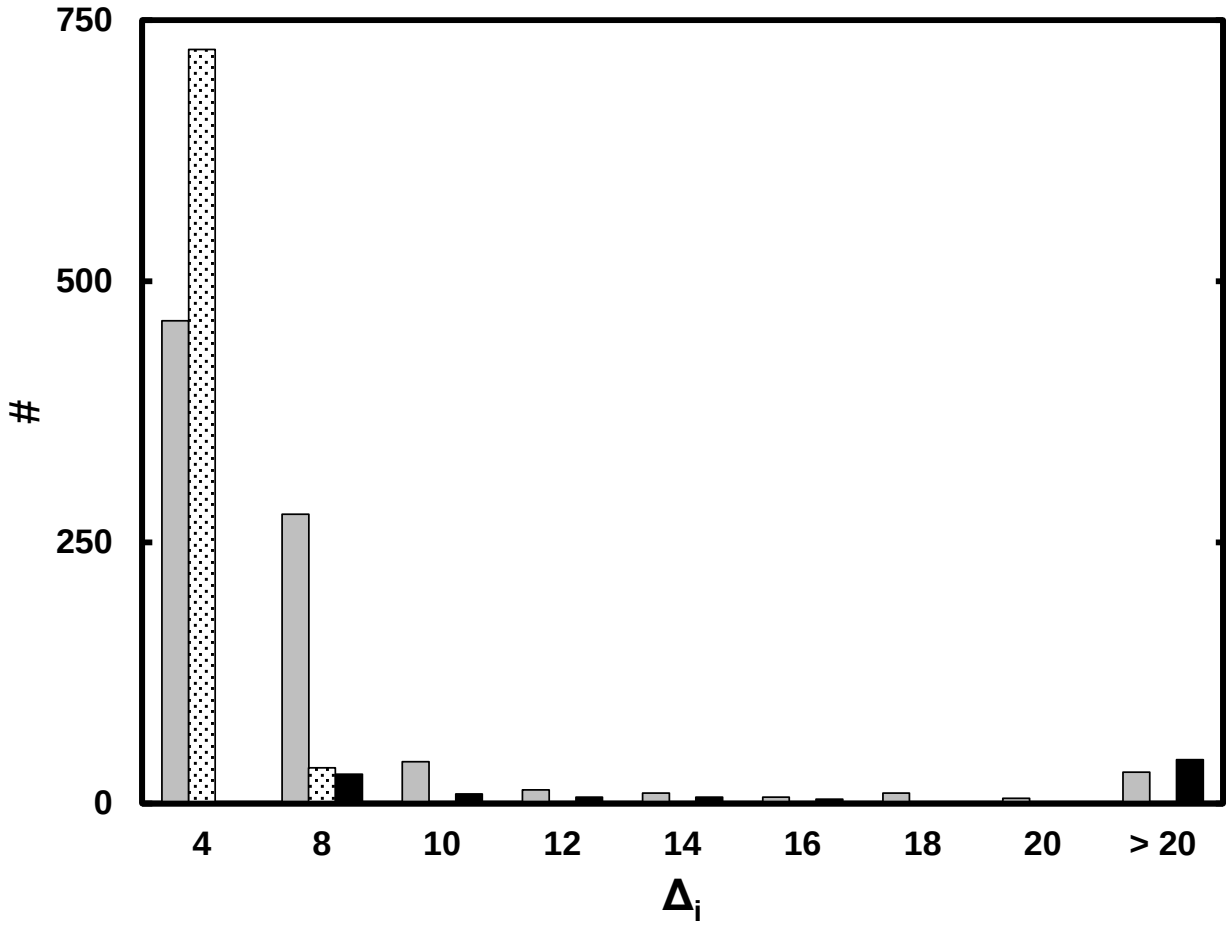

Figure 8. Viscosity η absolute percentage deviation Δ_i histogram: solid grey bar (Equation 10), regression with relative objective function; dot bar, regression with relative objective function and point removal (Equation 12); solid black bar, identified outliers.

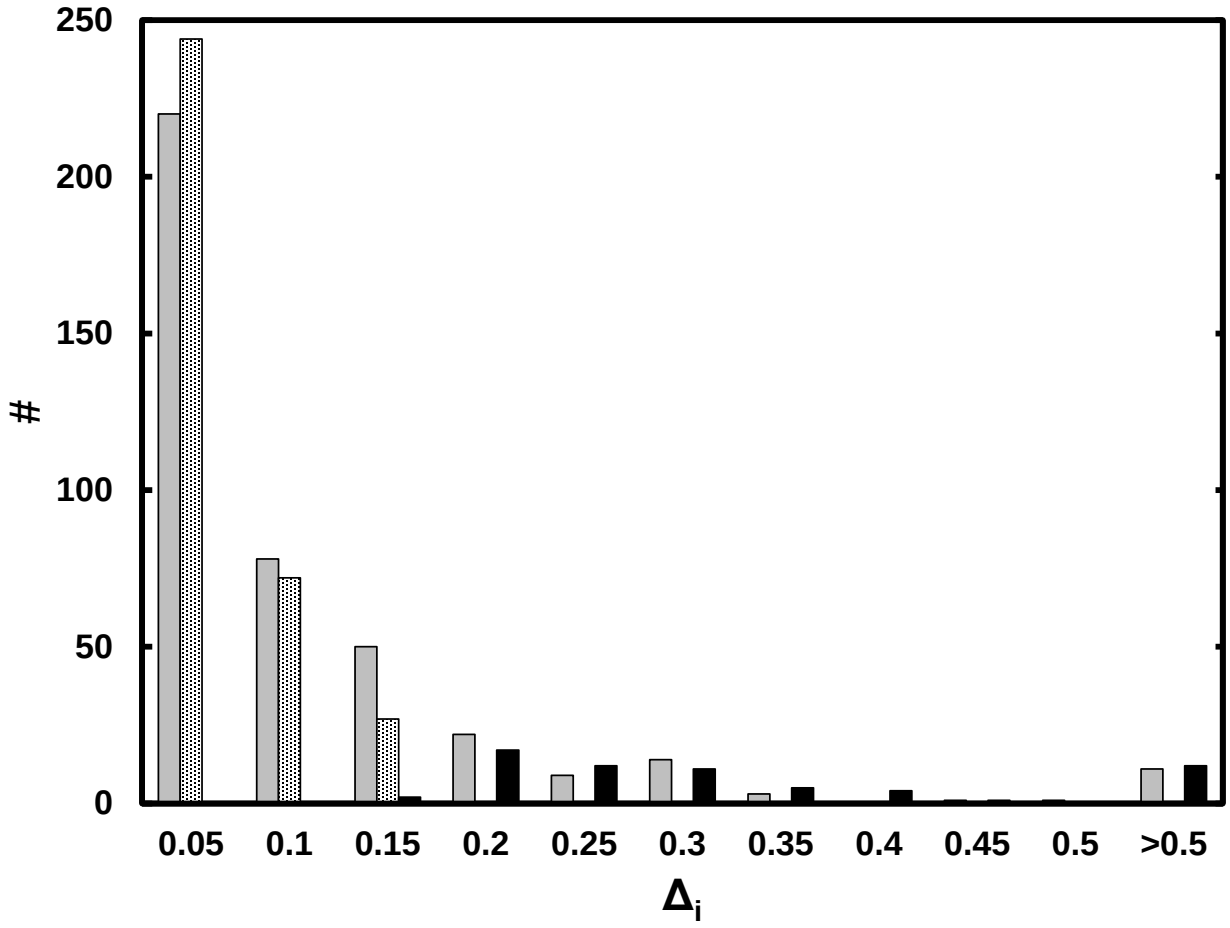

Figure 9. Density ρ absolute percentage deviation Δ_i histogram: solid grey bar (Equation 10), regression with relative objective function; dot bar, regression with relative objective function and point removal (Equation 12); solid black bar, identified outliers.

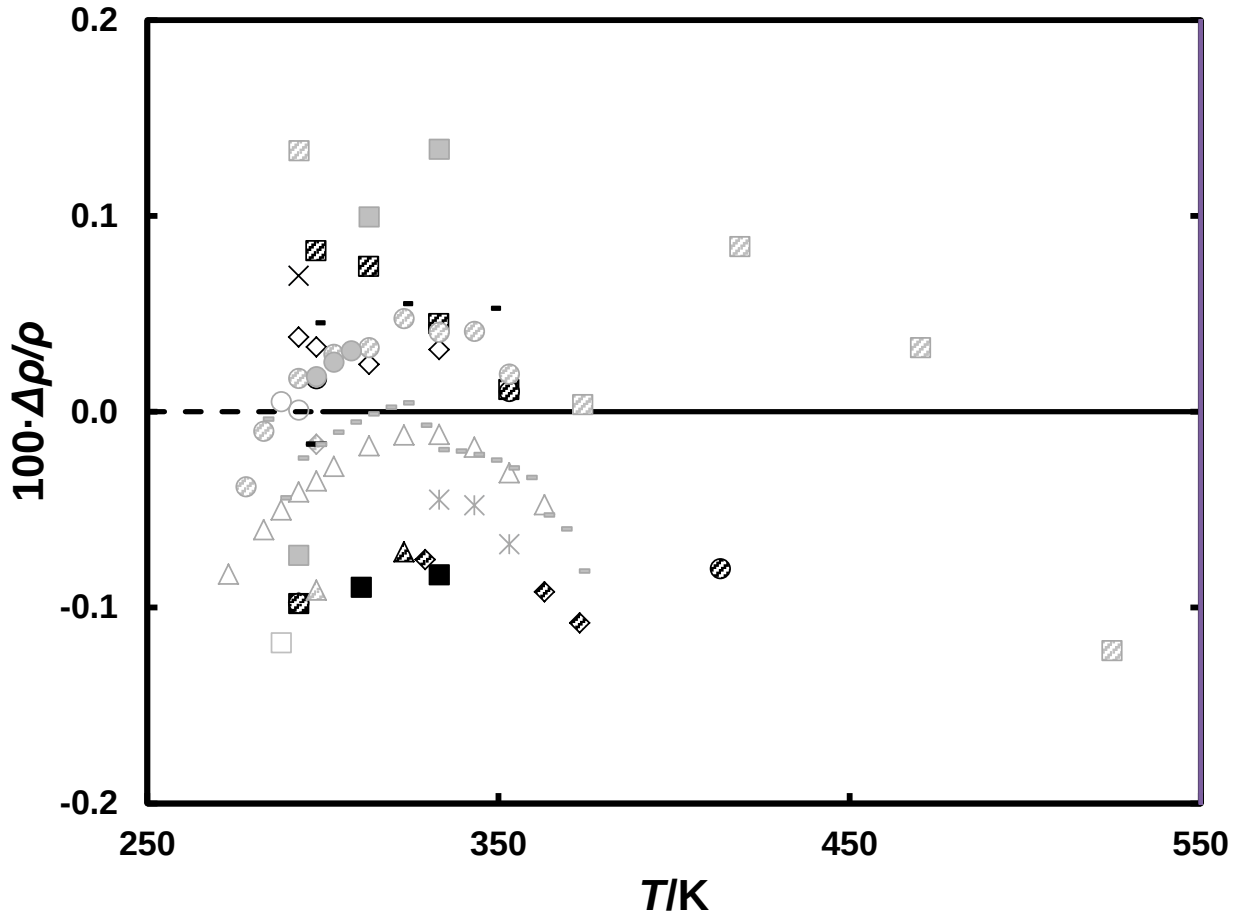

Figure 10. Relative deviations $\Delta\rho/\rho = \{\rho(\text{expt}) - \rho(\text{calc})\}/\rho(\text{calc})$ of the experimental density ρ(expt) at pressure P = 0.1 MPa for squalane from the value obtained in Equation (1) ρ(calc) as a function of temperature T: □,Tsujimoto[1]; ◇, Heilbron et al.[4]; ○, Tsujimoto[5]; ×, Sax and Stross[7]; ■, Whitmore et al.[8]; ✳, Cadogan and Purnell[9]; ▲, Cadogan et al.[10]; ▨, Kuss and Taslimi[11]; ◈, Laub and Purnell[12]; ◍, Kőrösi and Kováts[13]; ◬, Trejo et al.[14]; ▨, Graaf et al.[15]; ◇, Kumagai and Takahashi[16]; ○, Fermeglia and Torriano[17]; ◈, Lal et al.[18]; ◍, Fandiño et al.[19,20]; ▬, Tripathi[21]; ■, Kumagai et al.[22]; ●, Dubey and Sharma[24]; △, Harris[25]; ▬, Fandiño et al.[27]; ▬, Mylona et al.[28].

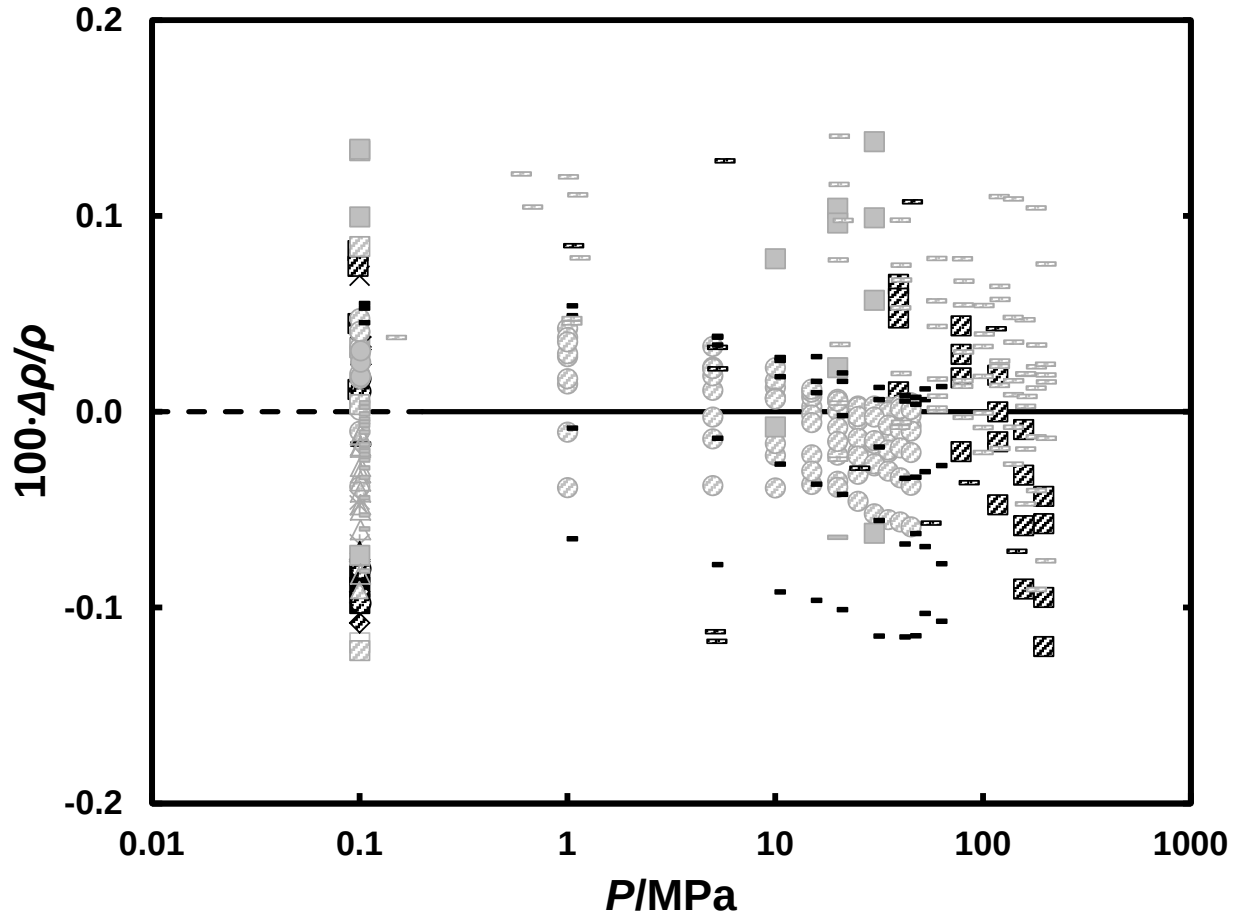

Figure 11. Relative deviations $\Delta\rho/\rho = \{\rho(\text{expt}) - \rho(\text{calc})\}/\rho(\text{calc})$ of the experimental density ρ(expt) at all temperatures T for squalane from the value obtained in Equation (1) ρ(calc) as a function of pressure P: □,Tsujimoto[1]; ◇, Heilbron et al.[4]; ○, Tsujimoto[5]; ×, Sax and Stross[7]; ■, Whitmore et al.[8]; ✳, Cadogan and Purnell[9]; ▲, Cadogan et al.[10]; ▨, Kuss and Taslimi[11]; ◈, Laub and Purnell[12]; ◍, Kőrösi and Kováts[13]; △, Trejo et al.[14]; ▨, Graaf et al.[15]; ◇, Kumagai and Takahashi[16]; ○, Fermeglia and Torriano[17]; ◈, Lal et al.[18]; ◍, Fandiño et al.[19,20]; ▬, Tripathi[21]; ■, Kumagai et al.[22]; ▬, Tomida et al.[23]; ▬, Ciotta et al.[26]; ●, Dubey and Sharma[24]; △, Harris[25]; ▬, Fandiño et al.[27]; ▬, Mylona et al.[28]; ▬, New Data.

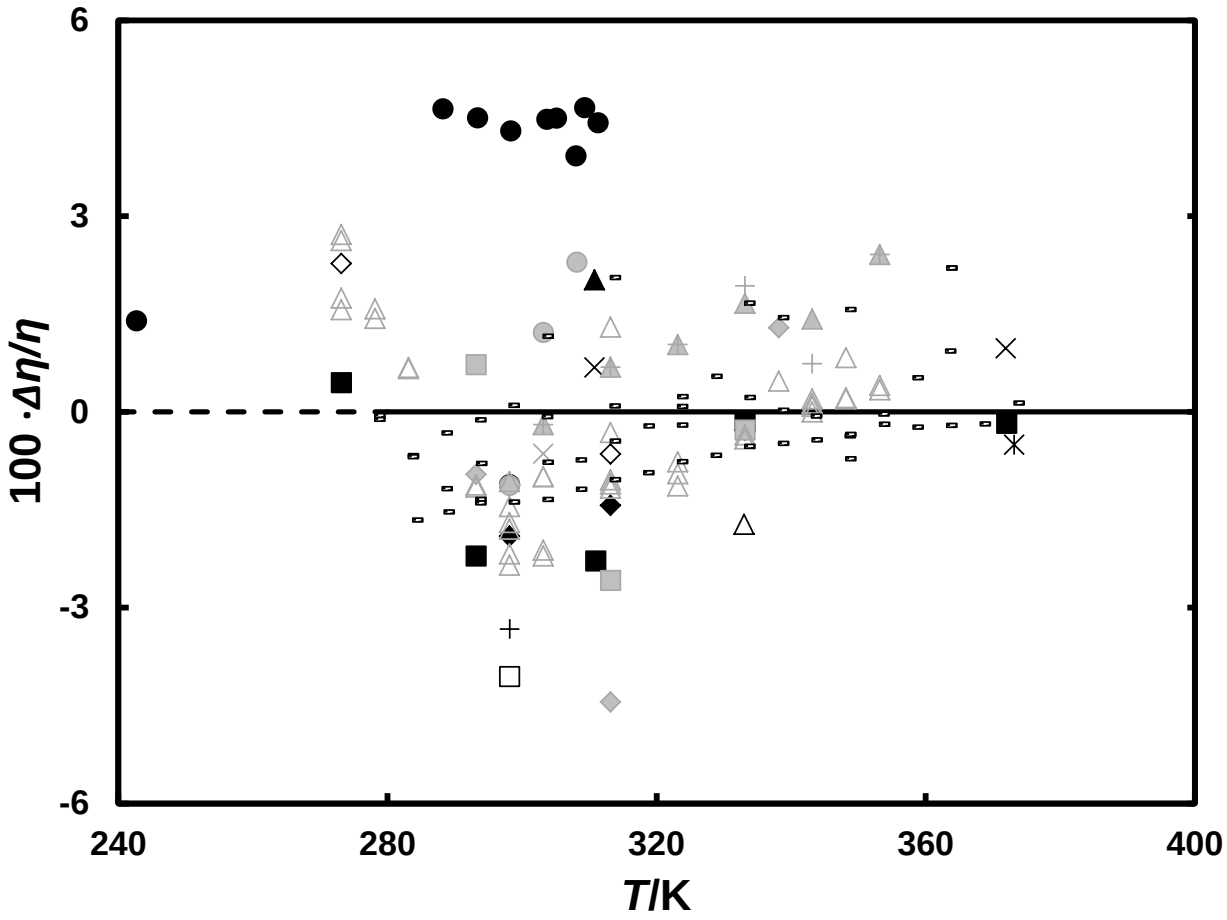

Figure 12. Relative deviations $\Delta\eta/\eta = \{\eta(\text{expt}) - \eta(\text{calc})\}/\eta(\text{calc})$ of the experimental viscosity η(expt) at pressure P = 0.1 MPa for squalane from the value obtained in Equation (4) η(calc) as a function of temperature T: ×, Sax and Stross[7]; ■, Whitmore et al.[8]; ◇, Kumagai and Takahashi[16]; ○, Fermeglia and Torriano[17]; ▩, Kumagai et al.[22]; ●, Dubey and Sharma[24]; △, Harris[25]; ▲, Sax and Stross[29]; ◆, Kuss and Golly[30]; ●, Barlow and Erginsav[31]; +, Jambon and Delmas[33]; △, Glowinkowski et al.[34]; □, Krahn and Luft[35]; ✳, Bair[36]; ×, Bair et al.[37]; ▲, Pensado et al.[38]; ◆, Bair[39]; +, Paredes et al.[40]; ▪, Comuñas et al.[41].

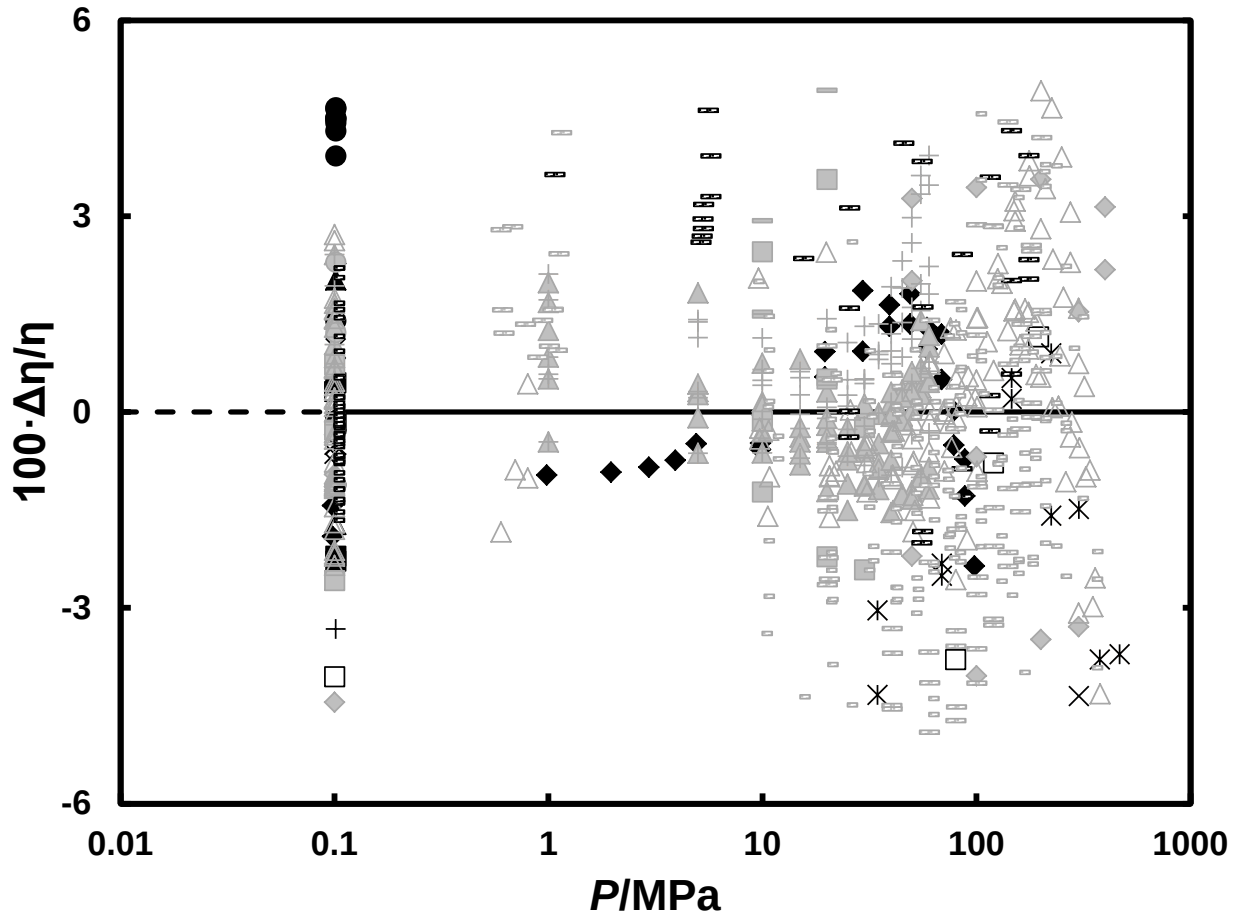

Figure 13. Relative deviations $\Delta\eta/\eta = \{\eta(\text{expt}) - \eta(\text{calc})\}/\eta(\text{calc})$ of the experimental viscosity η(expt) at all temperatures for squalane from the value obtained in Equation (4) η(calc) as a function of pressure P: ×, Sax and Stross[7]; ■, Whitmore et al.[8]; ◇, Kumagai and Takahashi[16]; ○, Fermeglia and Torriano[17]; ▒, Kumagai et al.[22]; ▬, Tomida et al.[23]; ●, Dubey and Sharma[24]; △, Harris[25]; ▬, Ciotta et al.[26]; ▲, Sax and Stross[29]; ◆, Kuss and Golly[30]; ●, Barlow and Erginsav[31]; +, Jambon and Delmas[33]; △, Glowinkowski et al.[34]; □, Krahn and Luft[35]; ✳, Bair[36]; ×, Bair et al.[37]; ▲, Pensado et al.[38]; ◆, Bair[39]; +, Paredes et al.[40]; ▬, Comuñas et al.[42]; ▬, Comuñas et al.[42]; ▬, New Data.

TOC Graphic.

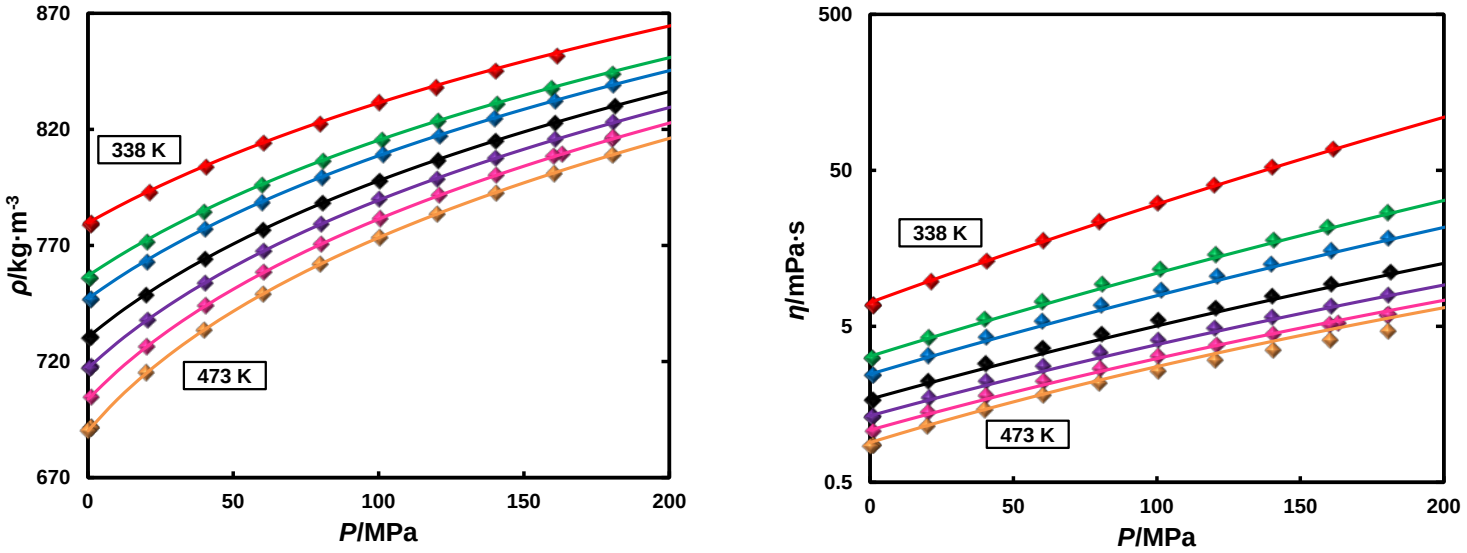

New Experimental Data and Reference Models for the Viscosity and Density of Squalane

Kurt A. G. Schmidt, Doug Pagnutti, Meghan D. Curran, Anil Singh, J. P. Martin Trusler, Geoffrey C. Maitland, Mark McBride-Wright